Earth and Planetary Science Letters 414 (2015) 30–44

Contents lists available at ScienceDirect

Earth and Planetary Science Letters

www.elsevier.com/locate/epsl

Partial melting of thickened continental crust in central Tibet: Evidence from geochemistry and geochronology of Eocene adakitic rhyolites in the northern Qiangtang Terrane

Xiaoping Long [a,b,*], Simon A. Wilde [c], Qiang Wang [a,b], Chao Yuan [a], Xuan-Ce Wang [c], Jie Li [a], Ziqi Jiang [a], Wei Dan [a]

[a] State Key Laboratory of Isotope Geochemistry, Guangzhou Institute of Geochemistry, Chinese Academy of Sciences, Guangzhou 510640, China
[b] CAS Center for Excellence in Tibetan Plateau Earth Sciences, Beijing 100101, China
[c] Department of Applied Geology, Curtin University, Perth, WA 6845, Australia

ARTICLE INFO

Article history:
Received 17 July 2014
Received in revised form 5 January 2015
Accepted 6 January 2015
Available online 22 January 2015
Editor: A. Yin

Keywords:
Tibetan Plateau
adakite
geochemistry
partial melting
northern Qiangtang Terrane

ABSTRACT

The composition of the deep crust is a key to understanding the formation of the low-velocity zone in the middle to lower crust of the Tibetan Plateau. The Suyingdi rhyolites exposed in the northern Qiangtang Terrane have high Sr (296–384 ppm) and low Y (5.81–7.93 ppm), with therefore high Sr/Y ratios (42–56), showing geochemical features of adakitic rocks. Zircon U–Pb dating yields an eruption age of 38.2±0.8 Ma (MSWD = 0.78). These adakitic rhyolites are high-K calc-alkaline in composition, displaying a weakly peraluminous character. They have low MgO content (0.20–0.70 wt.%) and $Mg^{\#}$ values (24–39), as well as low Sc (2.25–2.76 ppm), Cr (8–14 ppm), Co (1.6–3.5 ppm) and Ni (2–3 ppm) concentrations. The rocks are LREE-enriched ($(La/Yb)_N$ = 50–62) and display weakly negative Eu anomalies (Eu/Eu^* = 0.82–0.95) and pronounced negative Nb and Ta anomalies. They have low initial $(^{87}Sr/^{86}Sr)_i$ ratios (0.707860 to 0.708342) and enriched Nd isotopic compositions with $\varepsilon_{Nd}(t)$ values ranging from −8.4 to −5.0, which are indistinguishable from those of Cenozoic potassic and ultra-potassic lavas exposed in northern Tibet. Their much higher SiO_2 and lower Fe_2O_3 contents, yet similar MgO, Cr, Co, Ni, and $Mg^{\#}$ values to the potassic and ultra-potassic lavas, however, indicate that the rhyolites are unlikely to have formed by fractional crystallization of these lavas. Because of their low Nb/Ta ratios and similar Sr–Nd isotopic compositions to granulite xenoliths within the Cenozoic potassic rocks, we infer that the Suyingdi adakitic rhyolites were most likely produced by partial melting of a thickened lower crust in the garnet stability field. The magma source is most likely dominated by granulite facies metabasalts and clay-poor metamorphosed sedimentary rocks which indicate that the lower crust of northern Tibet is heterogeneous. In combination with data from previously-reported peraluminous and metaluminous adakitic rocks in the same region, the age and petrogenesis of the Suyingdi adakitic rhyolites suggest that the low-velocity zone in the deep crust of central and northern Tibet was most likely the result of partial melting of thickened crust.

1. Introduction

The Tibetan Plateau is generally considered to have formed in the early Cenozoic as a consequence of the continental collision between India and Asia along the Indus–Tsangpo suture (Molnar et al., 1993; Nelson et al., 1996; Owens and Zandt, 1997; Yin, 2000, 2006; Yin and Harrison, 2000; DeCelles et al., 2002; Chung et al., 2005; Ding et al., 2005). Uplift of the Tibetan Plateau during the last ~65 Ma has not only changed the global climate, but also irrevocably affected the isotopic composition of global oceans (Raymo and Ruddiman, 1992; Turner et al., 1996; Ruddiman, 1998; Chung et al., 1998; Dupont-Nivet et al., 2007). Although the time and mechanism of uplift still remain unclear (Molnar et al., 1993; Coleman and Hodges, 1995; Turner et al., 1996; Chung et al., 1998; Rowley, 1998; Roger et al., 2000; Tapponnier et al., 2001; Blisniuk et al., 2001; Harris, 2006), there is a distinction in radiogenic isotopic compositions of the Cenozoic lithosphere-derived igneous rocks exposed in southern and northern Tibet (Coulon et al., 1986; Arnaud et al., 1992; Turner et al., 1996; Miller et al., 1999; Hacker et al., 2000; Williams et al., 2001, 2004; Chung et al., 2003; Ding et al., 2003, 2007; Hou et al., 2004; Wang et al., 2005, 2008, 2012;

* Corresponding author. Tel.: +86 20 8529 0907.
E-mail address: longxp@gig.ac.cn (X. Long).

http://dx.doi.org/10.1016/j.epsl.2015.01.007
0012-821X/

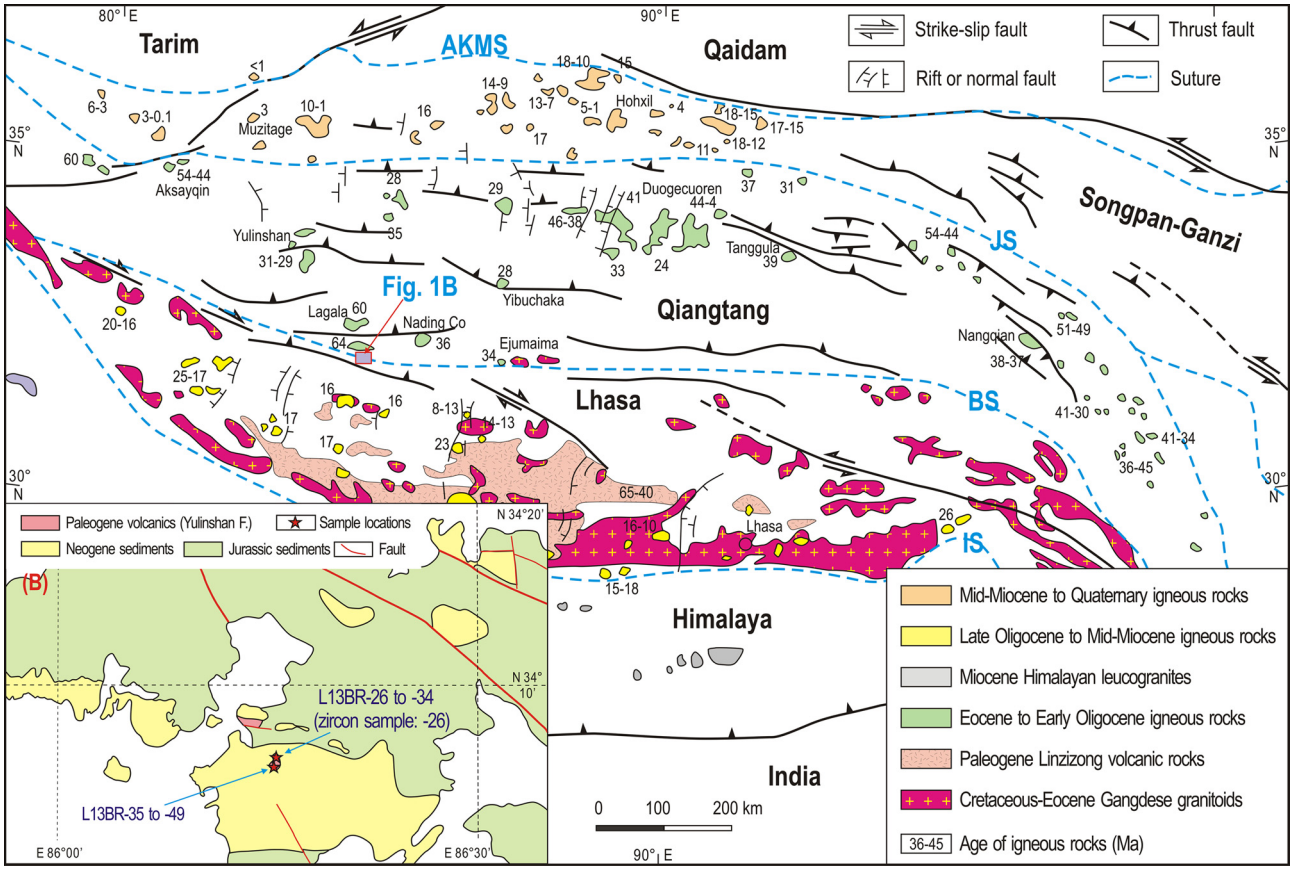

Fig. 1. Simplified geological map of the Tibetan Plateau showing major blocks and temporal-spatial distribution of Cenozoic volcanic rocks (after Yin and Harrison, 2000; Chung et al., 2005). Ages shown for volcanic rocks are from Ding et al. (2003, 2007), Chung et al. (2005), Guo et al. (2006), Wang et al. (2008), and references therein. Main suture zones between major blocks: AKMS, Anyimaqen–Kunlun–Muztagh; JS, Jinshajiang; BS, Bangong; IS, Indus. Major faults: MBT, Main Boundary Thrust. The inset geologic map shows outcrops of Cenozoic rhyolites at Suyingdi, northern Qiangtang Terrane, with location of samples used in this study.

Guo et al., 2006, 2007, 2013; Gao et al., 2007, 2008, 2010; Mo et al., 2007; Holbig and Grove, 2008; Ji et al., 2009; Zhao et al., 2009; Chen et al., 2010). The isotopic characteristics of the magma sources in southern Tibet are commonly considered to record northward subduction of the Indian continental lithosphere, whereas those in northern Tibet are likely produced by the southward subduction of Asian continental lithosphere (Yin and Harrison, 2000; Tapponnier et al., 2001; Chung et al., 2005; Yin, 2006; Ding et al., 2007; Nábělek et al., 2009).

However, a large number of geophysical studies have demonstrated that there is a widespread low-velocity zone in the middle to lower crust across the whole Tibetan Plateau (Nelson et al., 1996; Owens and Zandt, 1997; Yuan et al., 1997; Zhao et al., 2001; Wei et al., 2001; Unsworth et al., 2005; Le Pape et al., 2012). This low-velocity zone is commonly interpreted as a partially-molten zone and its distribution seems not to have been affected by the differences in tectonic mechanisms between southern and northern Tibet. Although several models have been proposed to interpret the formation of the molten zone, none of them is universally accepted (Wei et al., 2001; Unsworth et al., 2005; Caldwell et al., 2009; Bai et al., 2010; Zhang and Klemperer, 2010). The Cenozoic igneous rocks exposed in Tibet are dominantly from mantle sources, and so the general lack of crustal-derived igneous rocks has impeded greater insight into the formation of the molten zone (Roger et al., 2000; Tapponnier et al., 2001; Chung et al., 2005; Spurlin et al., 2005).

In order to constrain the composition of the deep crust, we present new geochronological and geochemical data for Cenozoic rhyolites exposed in the northern Qiangtang Terrane (Fig. 1). Our results demonstrate that the Eocene rhyolites are adakitic rocks that have been produced by partial melting of a thickened lower crust, thus providing new constraints on the middle to lower crust of central Tibet.

2. Geological background and sample descriptions

The Tibetan Plateau consists mainly of three east–west-trending terranes which are, from north to south, the Songpan–Ganzi, Qiangtang and Lhasa terranes (Fig. 1; Yin and Harrison, 2000; Chung et al., 2005; Ding et al., 2007). The Qiangtang Terrane is separated from the Songpan–Ganzi Terrane by the Jinshajiang suture, whereas it is separated by the Bangong suture from the Lhasa Terrane to the south, representing the final closure of the Paleo- and Meso-Tethyan oceans, respectively (Yin and Harrison, 2000; Ding et al., 2003). It is generally accepted that the formation of the Jinshajiang suture predates the Jurassic (Tapponnier et al., 2001), whereas the Bangong ocean opened during the Permian–Triassic (Sengör, 1984) or Early Jurassic (Yin et al., 1988) and closed prior to the Early Cretaceous (Murphy et al., 1997).

The Qiangtang Terrane is divided into two parts by an east–west-trending blueschist-bearing tectonic mélange (Kapp et al., 2000; Ding et al., 2003). The mélange was originally considered to be a suture zone separating the northern Qiangtang Terrane of Cathaysian affinity from the southern Qiangtang Terrane of Gondwanan affinity (Li et al., 1995). However, it has been more recently interpreted as a metamorphic core complex produced by underthrusting of oceanic crust and its sedimentary cover beneath the Qiangtang Terrane during the Early Mesozoic by southward-directed low-angle subduction along the Jinshajiang suture, only to be exhumed in an intracontinental setting by Late Triassic–

Early Jurassic normal faulting (Kapp et al., 2000, 2003). In the northern Qiangtang Terrane, Cenozoic volcanic rocks are extensively developed and dominated by potassic and ultra-potassic lavas formed at 45–27 Ma (Ding et al., 2003, 2007), some of which contain mafic and felsic granulite xenoliths (Hacker et al., 2000; Jolivet et al., 2003; Lai et al., 2011). These rocks are mostly shoshonitic in composition and mainly exposed in the Duogecuoren and Zhentouya areas (Fig. 1; Deng, 1998; Guo et al., 2006). It has been suggested that the geochemical characteristics of the potassic and ultra-potassic lavas are controlled by the composition of an enriched asthenospheric mantle source, the degree of partial melting of that source, and the combined processes of crustal assimilation and fractional crystallization (AFC) (Guo et al., 2006). A recent investigation, however, demonstrated that most of these lavas are high-K calc-alkaline andesites, dacites and rhyolites with geochemical characteristics of adakites, and thus are considered to represent partial melting of subducted sediment-dominated continental crust of the Songpan–Ganzi Terrane (Wang et al., 2008). Volcanic rocks of similar age are also exposed in the Yulinshan, Fenghuoshan–Nangqian and Tanggula areas (Wang et al., 2001; Ding et al., 2003; Chung et al., 2005; Guo et al., 2006). In the southern Qiangtang Terrane, Cenozoic volcanic rocks are locally exposed in the Nading Co, Ejumaima, Shuanghu and Siling Co areas, with eruption ages between 65 Ma and 28 Ma (Ding et al., 2007). These lavas are mostly Na-rich and calc-alkaline in composition and are considered to be derived from a primitive mantle source metasomatized by partial melts of metasedimentary lower crustal rocks (Ding et al., 2007).

To the north, the Songpan–Ganzi Terrane is characterized by a huge volume of Triassic terrigenous sediments that were deposited on continental and oceanic crust and derived mostly from the Triassic Qinling–Dabie orogen (Bruguier et al., 1997). The occurrence of non-marine sediments within this terrane defines the final accretion of the Qiangtang Terrane to the Eurasian margin along the Jinshajiang suture during the earliest Jurassic (Li et al., 1995; Yin and Harrison, 2000). Cenozoic volcanic rocks in the Songpan–Ganzi Terrane are volumetrically minor, but widely distributed (Fig. 1). They are mainly mafic and potassic to ultra-potassic in composition, and range in age from 17 Ma to Recent (Turner et al., 1993, 1996; Deng, 1998; Cooper et al., 2002; Guo et al., 2006). Some acidic lavas have also been discovered in this terrane, including the ~4 Ma rhyolites in the Ulugh Muztagh area and 18–15 Ma K-rich adakitic volcanic rocks in the Hohxil area (McKenna and Walker, 1990; Wang et al., 2005; Guo et al., 2006).

To the south, the Lhasa Terrane was shortened by ~180 km in response to the Indian–Asian collision and underwent an Andean-type orogeny prior to the collision (Murphy et al., 1997; Yin and Harrison, 2000; Tapponnier et al., 2001). It is characterized by voluminous calc-alkaline volcanic rocks of the Paleocene Linzizong volcanic suite (Miller et al., 2000; Zhou et al., 2004; Mo et al., 2007, 2008) and by huge calc-alkaline granitoids of the Tertiary Gangdese Batholith (Debon et al., 1986; Mo et al., 2005; Zhu et al., 2008; Ji et al., 2009). Published radiometric ages for the volcanic and intrusive rocks demonstrate that magmatism started in the Early Cretaceous (~130 Ma) and lasted until the Late Eocene (~40 Ma), with a distinct time gap between ~75 and 60 Ma (Coulon et al., 1986; Debon et al., 1986; Harrison et al., 1997; Murphy et al., 1997; Miller et al., 1999; Wen et al., 2008). The Linzizong volcanic rocks are widely distributed in the southern Lhasa Terrane and consist mainly of calc-alkaline andesitic lavas, tuffs and breccias, with dacitic to rhyolitic ignimbrites (Miller et al., 2000; Mo et al., 2008). Isotopic dating of the volcanic rocks near Lhasa has yielded eruption ages between 60 Ma and 49 Ma and revealed a westward younging trend (Miller et al., 2000; Zhou et al., 2004). Geochemical studies suggest that the Linzizong volcanic rocks were produced by subduction of the Neo-Tethys Ocean (Mo et al., 2007). Overlying the Linzizong volcanics, Miocene potassic to ultra-potassic lavas (24–8 Ma) are sporadically exposed in the southern Lhasa Terrane and it is commonly considered that they formed as a result of slab break-off beneath southern Tibet (Davies and von Blanckenburg, 1995; Miller et al., 1999; Chemenda et al., 2000; Williams et al., 2004; Ding et al., 2007). The Gangdese Batholith is mainly composed of dioritic plutons formed in the Cretaceous to Tertiary (Harris et al., 1988; Mo et al., 2005; Ji et al., 2009). Formation of the Gangdese Batholith is attributed to northward subduction of the Neo-Tethys ocean floor beneath the Lhasa Terrane along the Indus suture, but prior to the Indian–Asian collision (>50 Ma) (Debon et al., 1986; Mo et al., 2005; Zhu et al., 2008). In addition to the Gangdese Batholith, some post-collisional (26.2–10.1 Ma) adakitic intrusive rocks are also present in the Lhasa Terrane and are generally interpreted to be produced by partial melting of thickened mafic lower crust (Chung et al., 2003; Hou et al., 2004; Guo et al., 2007), although a few workers ascribe their petrogenesis to partial melting of subducted oceanic crust (Qu et al., 2004).

In this study, our samples were collected from the volcanic rocks exposed in the Suyingdi area in the northern Qiangtang Terrane. The lavas consist mainly of high-K rhyolites that erupted at two locations, uncomfortably overlying Jurassic and Neogene sediments (Fig. 1). The rhyolites show typical porphyritic texture (Figs. 2a–b), with the phenocrysts mostly consisting of anhedral quartz and euhedral feldspar with embayed crystal margins. The feldspar phenocrysts are dominated by plagioclase (andesine to labradorite), with some K-feldspar. Most display twinning or zoning (Figs. 2b–c) and reaction rims are commonly present at the margin of plagioclase phenocrysts (Fig. 2d). In some samples, there are a few euhedral biotite phenocrysts that have been partly converted to chlorite (Figs. 2a–b). The matrix is mainly composed of tiny crystals of plagioclase, K-feldspar, and quartz, with minor volcanic glass.

3. Analytical methods

Major and trace elements of twenty-three samples were analyzed using a Rigaku ZSX100e Xray fluorescence spectrometer and a Perkin-Elmer Sciex ELAN 6000 ICP-MS, respectively (online Appendix A, Supplementary Table 1). One sample (L13BR26) were separated from for zircon U–Pb dating and dated by an Agilent 7500a ICP-MS with a pulsed Resonetic 193 nm ArF excimer laser (online Appendix A, Supplementary Table 2). The whole-rock Sr–Nd and Pb isotopes of eight volcanic samples were analyzed using a Micromass Isoprobe multi-collector inductively-coupled plasma mass spectrometer (MC-ICP-MS) and a NEPTUNE MC-ICP-MS, respectively (Table 1). Except for Pb isotopic analyses were determined at the ALS Chemex (Guangzhou) Co Ltd, other analyses were accomplished at the State Key Laboratory of Isotope Geochemistry, Guangzhou Institute of Geochemistry, Chinese Academy of Sciences. The Detailed analytical procedures are attached in online Appendix B, Analytical methods.

4. Results

4.1. Whole-rock geochemistry

The volcanic samples are characterized by uniform geochemical compositions and record high SiO_2 contents ranging from 70.43 wt.% to 72.02 wt.% (Supplementary Table 1). They have high K_2O (3.53–3.74 wt.%) and slightly lower Na_2O (2.98–3.55 wt.%) contents, thus recording relatively high K_2O/Na_2O ratios (1.01–1.21), indicating that they are high-K calc-alkaline lavas (Fig. 3a). The rocks are subalkaline, and nearly all of them plot in the field

Fig. 2. Textural features of the Suyingdi rhyolites from the northern Qiangtang Terrane: (a) under plane-polarized light and (b–d) under cross-polarized light, showing flow alignment with phenocrysts dominated by anhedral quartz and euhedral plagioclase (andesine to labradorite), with minor K-feldspar and biotite. The abbreviations for minerals: Qz, quartz; Pl, plagioclase; Kf, K-feldspar; Bi, biotite; Chl, chlorite.

of rhyolite in the TAS discrimination diagram (Fig. 3b). Compared with the Hohxil K-rich adakitic volcanic rocks in the Songpan–Ganzi Terrane (Wang et al., 2005), the rocks display slightly lower Al_2O_3 (14.74–15.41 wt.%), and much lower CaO (2.25–2.76 wt.%), and MgO (0.20–0.70 wt.%) contents and $Mg^{\#}$ values (24–39) (Fig. 3c). The ASI index (A/CNK = $[Al_2O_3/(CaO + Na_2O + K_2O)$ mol%]) varies from 1.03 to 1.16, defining a weakly peraluminous character (Fig. 3d).

The rhyolite samples have low Sc = 2.3–2.8 ppm, Cr = 8–14 ppm, Co = 2–3 ppm and Ni = 2–3 ppm, which are much lower than those of the Hohxil K-rich adakitic rocks (Wang et al., 2005). The rhyolites have relatively high Sr (296–384 ppm) and low Y (5.81–7.93 ppm) concentrations, and thus show high Sr/Y ratios (42–56), which are similar to those of average adakite, but different from those of normal Phanerozoic arc igneous rocks (Condie, 2005). The rhyolites are also LREE-enriched ($(La/Yb)_N$ = 50–62) and display weakly negative Eu anomalies (Eu/Eu^* = 0.82–0.95) (Fig. 4a), with pronounced negative Nb and Ta anomalies, and marked positive Pb spikes in the primitive mantle-normalized trace element variation diagram (Fig. 4b).

4.2. Zircon U–Pb ages

Twenty-five zircons from rhyolite sample L13BR26 were analyzed to constrain the formation age of the volcanic rocks. The zircon grains are transparent and prismatic with lengths ranging from 100 to 220 μm and widths from 80 to 110 μm. In CL images, they display well-developed concentric oscillatory zoning (Fig. 5). The zircons have high Th/U ratios (0.93–1.66), which, together with the concentric oscillatory zoning, indicate an igneous origin. The twenty-five zircon grains are concordant and yield almost identical $^{206}Pb/^{238}U$ ages between 32.5 Ma and 42.2 Ma (Supplementary Table 2), with a weighted mean age of 38.2 ± 0.8 Ma (MSWD = 0.78), representing the time of eruption of the rhyolitic lava.

4.3. Sr–Nd–Pb isotopic compositions

Eight samples were analyzed for Sr–Nd isotopes and they display variable $^{87}Rb/^{86}Sr$ ratios from 1.2244 to 1.4473, with the measured $^{87}Sr/^{86}Sr$ ratios varying between 0.707861 and 0.708343. Using the formation age of the rhyolite (38.2 Ma), the calculated initial $(^{87}Sr/^{86}Sr)_i$ ratios range from 0.707860 to 0.708342 (Table 1), which is consistent with the published data for Cenozoic volcanic rocks in the Songpan–Ganzi and northern Qiangtang terranes (Fig. 6) (Ding et al., 2003; Wang et al., 2005, 2008), but lower than that of granulite xenoliths discovered within the Cenozoic (ultra-)potassic lavas in the northern Qiangtang Terrane (Lai et al., 2011). The $^{147}Sm/^{144}Nd$ ratios range from 0.0889 to 0.0917 and their measured $^{143}Nd/^{144}Nd$ ratios vary between 0.512180 and 0.512354 (Table 1). Because all of the samples have $f_{Sm/Nd}$ ratios between −0.54 and −0.53, one stage Nd isotopic model ages (T_{DM}) are used in the discussion. One sample (L13BR29) has a low calculated initial $\varepsilon_{Nd}(t)$ value of −8.4 and old T_{DM} model age of 1206 Ma. The rest of the volcanic samples show similar $\varepsilon_{Nd}(t)$ values, ranging from −5.3 to −5.0, with T_{DM} model ages between 976 Ma and 1010 Ma. The Nd isotopic characteristics are consistent with the Cenozoic volcanic rocks in the Songpan–Ganzi and northern Qiangtang Terrane (Ding et al., 2003; Wang et al., 2005, 2008), but lower than those of the calc-alkaline lavas exposed in the southern Qiangtang Terrane and the 18–12 Ma adakitic rocks of the Lhasa Terrane (Hou et al., 2004; Ding et al., 2007) (Fig. 6).

For the Pb isotopes, the rhyolite samples are characterized by radiogenic Pb with ranges of $^{206}Pb/^{204}Pb$ (18.348–18.626), $^{207}Pb/^{204}Pb$ (15.708–15.723), and $^{208}Pb/^{204}Pb$ (38.610–38.695).

Table 1
Sr–Nd–Pb isotopic composition of the Suyingdi rhyolites.

Sample	Rb	Sr	$\frac{^{87}Rb}{^{86}Sr}$	$\frac{^{87}Sr}{^{86}Sr} \pm 2\sigma$	$\left(\frac{^{87}Sr}{^{86}Sr}\right)_i$	$f_{Rb/Sr}$	Sm	Nd	$\frac{^{147}Sm}{^{144}Nd}$	$\frac{^{143}Nd}{^{144}Nd} \pm 2\sigma$	$\left(\frac{^{143}Nd}{^{144}Nd}\right)_i$	$\varepsilon_{Nd}(t)$	$T_{DM\text{-}1}$	$f_{Sm/Nd}$	$\frac{^{206}Pb}{^{204}Pb} \pm 2\sigma$	$\frac{^{207}Pb}{^{204}Pb} \pm 2\sigma$	$\frac{^{208}Pb}{^{204}Pb} \pm 2\sigma$	$\left(\frac{^{206}Pb}{^{204}Pb}\right)_i$	$\left(\frac{^{207}Pb}{^{204}Pb}\right)_i$	$\left(\frac{^{208}Pb}{^{204}Pb}\right)_i$
L13BR27	156	311	1.4473	0.708061 ± 16	0.708060	16.74	3.30	21.96	0.0910	0.512342 ± 8	0.512320	−5.3	1004	−0.54	18.923 ± 5	15.738 ± 3	39.555 ± 22	18.499	15.716	38.689
L13BR29	163	384	1.2244	0.708343 ± 14	0.708342	14.00	3.33	22.09	0.0913	0.512180 ± 8	0.512157	−8.4	1206	−0.54	18.890 ± 4	15.738 ± 2	39.484 ± 16	18.503	15.718	38.661
L13BR31	165	338	1.4100	0.708105 ± 16	0.708104	16.28	3.39	23.11	0.0889	0.512351 ± 8	0.512328	−5.1	976	−0.55	18.912 ± 3	15.739 ± 2	39.517 ± 12	18.473	15.716	38.610
L13BR33	164	330	1.4376	0.707973 ± 18	0.707972	16.62	3.23	21.50	0.0910	0.512354 ± 8	0.512332	−5.0	989	−0.54	18.870 ± 4	15.736 ± 3	39.539 ± 20	18.626	15.723	38.653
L13BR35	158	338	1.3510	0.707946 ± 14	0.707945	15.56	3.20	21.15	0.0917	0.512349 ± 10	0.512326	−5.1	1001	−0.53	18.925 ± 1	15.739 ± 1	39.531 ± 7	18.522	15.718	38.695
L13BR38	156	347	1.3033	0.707970 ± 12	0.707969	14.97	3.17	21.20	0.0906	0.512349 ± 8	0.512326	−5.1	992	−0.54	18.913 ± 2	15.736 ± 1	39.508 ± 9	18.519	15.715	38.690
L13BR41	159	343	1.3377	0.707883 ± 12	0.707883	15.39	3.36	22.23	0.0917	0.512342 ± 10	0.512319	−5.3	1010	−0.53	18.894 ± 5	15.735 ± 3	39.465 ± 22	18.412	15.710	38.648
L13BR44	156	333	1.3611	0.707861 ± 14	0.707860	15.68	3.36	22.47	0.0905	0.512347 ± 6	0.512324	−5.2	993	−0.54	18.934 ± 5	15.739 ± 4	39.486 ± 22	18.348	15.708	38.646

$\left(\frac{^{87}Sr}{^{86}Sr}\right)_i = \left(\frac{^{87}Sr}{^{86}Sr}\right)_S - \left(\frac{^{87}Rb}{^{86}Sr}\right)_S (e^{\lambda t} - 1)$.
$f_{Rb/Sr} = \left(\frac{^{87}Rb}{^{86}Sr}\right)_S / \left(\frac{^{87}Rb}{^{86}Sr}\right)_{CHUR} - 1$.
$\varepsilon_{Nd}(t) = [(\frac{^{143}Nd}{^{144}Nd})_S / (\frac{^{143}Nd}{^{144}Nd})_{CHUR} - 1] \times 10\,000$.
$f_{Sm/Nd} = [(\frac{^{147}Sm}{^{144}Nd})_S / (\frac{^{147}Sm}{^{144}Nd})_{CHUR}] - 1$.
$T^1_{DM} = 1/\lambda_{Sm} \times \ln\{[(\frac{^{143}Nd}{^{144}Nd})_S - 0.51315]/[(\frac{^{147}Sm}{^{144}Nd})_S - 0.2137]\}$.
Where S = sample, $(\frac{^{147}Sm}{^{144}Nd})_{CHUR} = 0.512638$ and $(\frac{^{147}Sm}{^{144}Nd})_{CHUR} = 0.1967$.

They are more radiogenic than MORB and show ratios distinct from GLOSS (Average global subducted sediment composition) (Fig. 7). Unlike the Sr–Nd isotopes, the rhyolites exhibit Pb isotope compositions different from the Cenozoic ultra-potassic rocks in the Qiangtang Terrane (Ding et al., 2003). Although the rhyolites have moderate $^{206}Pb/^{204}Pb$ ratios, similar to the Cenozoic ultra-potassic rocks and the early Tertiary Linzizong volcanic rocks exposed in the Lhasa Terrane, their $^{207}Pb/^{204}Pb$ ratios are higher than those of the Linzizong volcanic rocks, whereas their $^{208}Pb/^{204}Pb$ ratios are lower than the ultra-potassic rocks (Figs. 7a–b). It is noteworthy that the Pb isotope compositions of the rhyolites are similar to those of the Cenozoic potassic rocks in the Songpan–Ganzi Terrane and overlap the fields of global marine sediments in conventional Pb isotope diagrams (Fig. 7).

5. Discussion

5.1. Petrogenesis of the Suyingdi adakitic rhyolites

The Suyingdi rhyolites have relatively high Sr (296–384 ppm), and low Y (5.81–7.93 ppm) and Yb (<0.58 ppm), thus giving high Sr/Y (42–56) and $(La/Yb)_N$ (50–62) ratios, indicating geochemical characteristics of adakitic rocks (Figs. 8a–b). Their adakitic nature is in contrast to other Cenozoic volcanic rocks in Tibet, as discussed above, although they are similar to the Duogecuoren adakitic rocks. Hence they are different from the potassic and ultra-potassic lavas, the Na-rich and calc-alkaline lavas and the strongly peraluminous rhyolites exposed in northern Tibet (McKenna and Walker, 1990; Deng, 1998; Jolivet et al., 2003; Ding et al., 2003, 2007; Wang et al., 2005, 2008, 2012; Guo et al., 2006). Several petrogenetic models have been proposed to interpret the origin of adakitic rocks, including: (1) melting of subducted oceanic crust, followed by interaction with the overlying mantle wedge (Defant and Drummond, 1990; Stern and Kilian, 1996; Rapp et al., 1999; Martin et al., 2005; Wang et al., 2007); (2) fractional crystallization of parental basaltic magmas with/without crustal assimilation (Prouteau and Scaillet, 2003; Macpherson et al., 2006); (3) magma mixing between felsic and basaltic magmas (Streck et al., 2007); (4) partial melting of delaminated lower crust (Kay and Kay, 1993; Xu et al., 2002; Wang et al., 2006); and (5) partial melting of thickened lower crust (Atherton and Petford, 1993; Chung et al., 2003; Hou et al., 2004).

The Suyingdi adakitic rhyolites are characterized by high SiO_2 (70.43–72.02 wt.%), low MgO (0.20–0.70 wt.%) and $Mg^{\#}$ (24–39), and similar amounts of K_2O and Na_2O (~3.5 wt.%), which are different from those of typical slab-derived adakites (Fig. 8c) (Martin et al., 2005). These geochemical features, in combination with their low Cr (8–14 ppm), Co (2–3 ppm) and Ni (2–3 ppm) contents, indicate an evolved magma source and exclude melt–mantle interaction that commonly occurs when slab-derived melt traverses mantle peridotite in the wedge above a subducting slab (Rapp et al., 1999; Smithies, 2000). Recent studies reveal that some primary adakitic magmas formed by crustal assimilation and fractional crystallization (AFC) processes of parental basaltic magmas and these show significant systematic variations in geochemistry and isotopic compositions (e.g., MgO, Cr, Ni contents and Sr–Nd isotopic values), and usually develop complex compositional zonation in the mafic minerals (e.g., amphibole and clinopyroxene) (Castillo et al., 1999). The uniform geochemistry and $\varepsilon_{Nd}(t)$ values of the rhyolite samples in this study, together with the absence of amphibole and clinopyroxene, do not support an origin from primary basaltic magma by AFC processes. This interpretation is supported by their REE concentrations, because the rhyolites have lower LREE concentrations and slightly higher La/Sm and $(La/Yb)_N$ ratios than those of the Cenozoic mantle-derived Na-rich and calc-alkaline lavas exposed in the southern Qiangtang Terrane

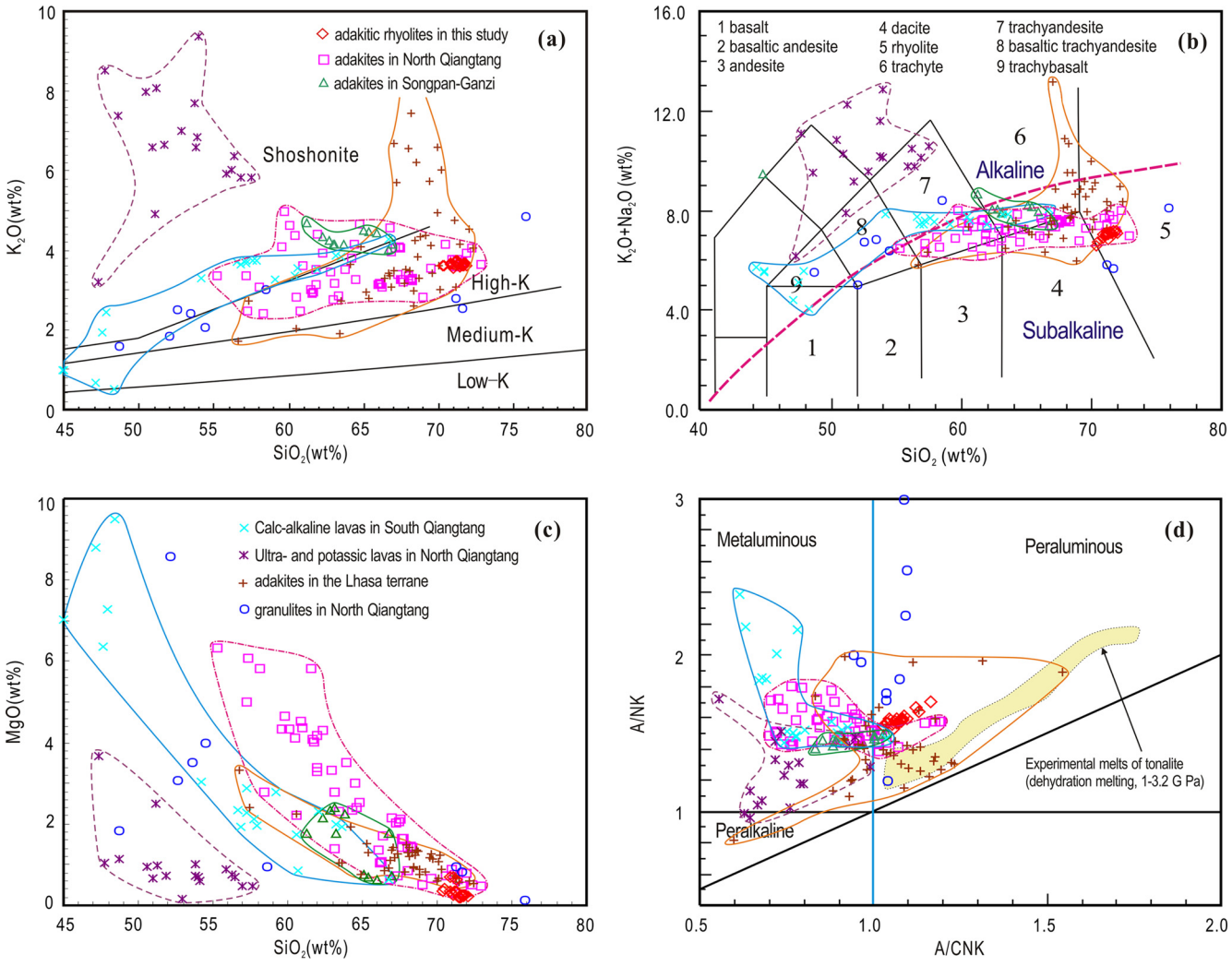

Fig. 3. Geochemical classification diagrams for the Suyingdi rhyolites: (a) K_2O–SiO_2; (b) total alkali (Na_2O+K_2O) versus SiO_2; (c) MgO–SiO_2 diagram; (d) ANK versus ACNK. Data sources are as follows: adakites in North Qiangtang (Lai et al., 2007; Wang et al., 2008); adakites in Songpan–Ganzi (Wang et al., 2005); calc-alkaline lavas in South Qiangtang (Ding et al., 2003, 2007); ultra-potassic and potassic lavas in North Qiangtang (Ding et al., 2003); adakites in Lhasa Terrane (Chung et al., 2003; Hou et al., 2004); granulies in North Qiangtang (Lai et al., 2011).

(Figs. 9a–b). The rhyolites show negative $\varepsilon_{Nd}(t)$ values (−8.4 to −5.0), which are significantly lower than those (−3.0 to +1.1) of the calc-alkaline lavas (Ding et al., 2007) and preclude a direct origin from the calc-alkaline lavas simply by fractional crystallization. The Sr–Nd isotopic compositions of the rhyolites are indistinguishable from those of the Cenozoic potassic and ultra-potassic lavas exposed in northern Tibet (Fig. 6) (Deng, 1998; Ding et al., 2003; Guo et al., 2006), but their much higher SiO_2 and lower Fe_2O_3 contents, and similar MgO, Cr, Co, Ni, and $Mg^{\#}$ values, indicate that the rhyolites are unlikely to have formed by fractional crystallization of the potassic or ultra-potassic lavas (Fig. 10). This is consistent with their REE concentrations, because there is no trend of fractional crystallization between the rhyolites and the Cenozoic potassic and ultra-potassic lavas (Fig. 9). The high SiO_2, simple mineralogy and absence of mafic xenoliths suggest that magma mixing between felsic and basaltic magmas is also not feasible for the formation of the adakitic rhyolites. Because adakitic rocks produced by partial melting of delaminated lower crust generally have high MgO, TiO_2, Fe_2O_3, Cr, Co, and Ni that increase during ascent of the magmas (Xu et al., 2002; Wang et al., 2006), the characteristics of low compatible trace elements of the Suyingdi rhyolites exclude an origin from partial melting of delaminated lower crust (Fig. 10). The low Nb/Ta and Zr/Sm ratios support amphibolite melting, but not eclogite melting (Fig. 8d).

Recent published Nd isotopic data for mafic and felsic granulites exposed in the northern Qiangtang Terrane (Lai et al., 2011) are comparable with the isotopic compositions of the Suyingdi rhyolites (Fig. 6). In combination with the adakitic characteristics, we suggest that the rhyolites were most likely produced by partial melting of thickened lower crust that consists of granulite facies rocks in the garnet stability field. We note that the rhyolites have relatively large variations in $Mg^{\#}$ (24–39). Because of their very low MgO contents (0.20–0.70 wt.%), we interpret the $Mg^{\#}$ variations as indicative of a heterogeneous magma source, including not only mafic, but also felsic granulites.

Because adakitic rocks (46–38 Ma) are exposed in the northern Qiangtang Terrane and are more mafic than the younger Suyingdi adakitic rhyolites (Lai et al., 2007; Wang et al., 2008), there is a possibility that the latter were produced by fractional crystallization of mafic minerals from these slightly earlier adakitic rocks. This fractional crystallization trend is illustrated in Fig. 10. However, such fractional crystallization is not supported by the REEs, because the earlier adakitic rocks plot with an opposite trend of higher La and Sm concentrations and slightly lower La/Sm, $(La/Yb)_N$ ratios than those of the Suyingdi rhyolites (Fig. 9). There-

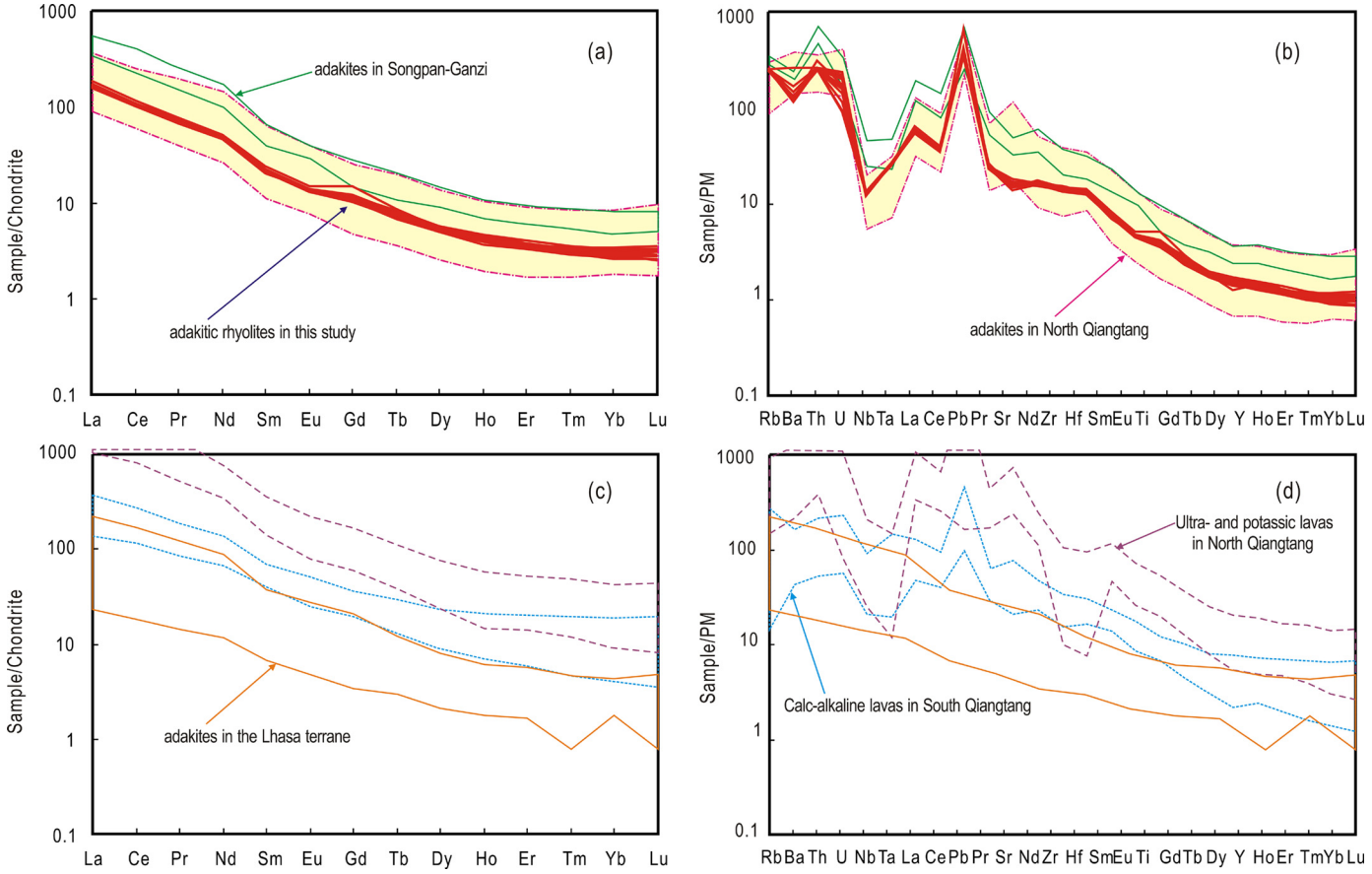

Fig. 4. (a) Chondrite-normalized REE patterns and (b) primitive mantle-normalized spider diagrams for the Suyingdi rhyolites. (c–d) Other representative Cenozoic igneous rocks in Tibet. Normalizing values are from Sun and McDonough (1989). Data source for other igneous rocks are as in Fig. 3.

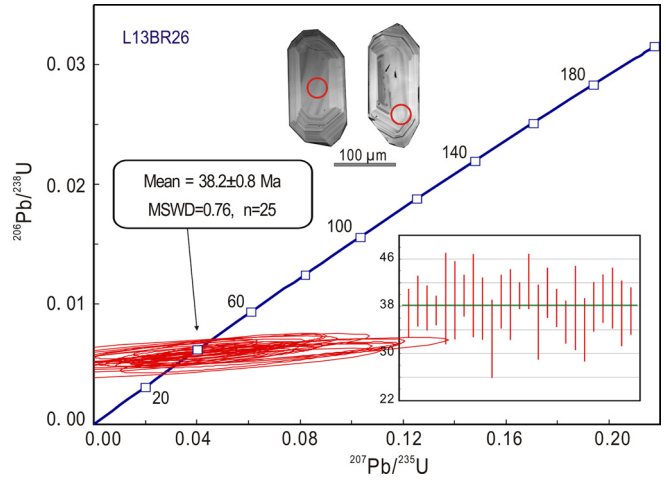

Fig. 5. U–Pb concordia diagram for zircons from sample L13BR26 from the Suyingdi rhyolite with representative CL images. The analytical sites are marked by red circles. (For interpretation of the references to color in this figure legend, the reader is referred to the web version of this article.)

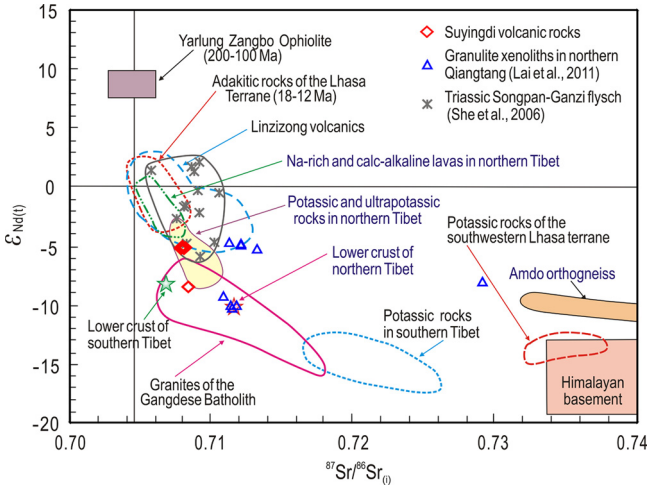

Fig. 6. Sr–Nd isotopic composition of the Suyingdi adakitic rhyolites. Data sources are as follows: Himalayan basement (Ahmad et al., 2000); Yarlung Zangbo Ophiolite (Miller et al., 2003; Xu and Castillo, 2004; Zhang et al., 2005); Na-rich and calc-alkaline lavas in northern Tibet (Deng, 1998; Ding et al., 2007); potassic and ultra-potassic lavas in northern Tibet (Ding et al., 2003); potassic rocks in southern Tibet (Zhao et al., 2009; Chen et al., 2010); potassic rocks of the southwestern Lhasa Terrane (Miller et al., 1999); adakitic rocks of the Lhasa Terrane (Chung et al., 2003; Hou et al., 2004; Gao et al., 2007; Guo et al., 2007); granites of the Gangdese Batholith (Mo et al., 2005); Amdo orthogneiss (Harris et al., 1988); Linzizong volcanics (Mo et al., 2007); Triassic Songpan–Ganzi flysch (She et al., 2006); lower crust of southern Tibet (Miller et al., 1999); and lower crust of northern Tibet (Lai et al., 2007).

fore, we suggest that the Suyingdi rhyolites were unlikely to be derived from the earlier adakitic rocks by fractional crystallization.

5.2. Composition of the lower crust below northern Tibet

The voluminous Cenozoic magmatic rocks exposed in northern Tibet are mostly mantle-derived and can not be used to trace the composition of the lower crust. They are dominated by potassic and ultra-potassic volcanic rocks that were most likely derived from an enriched mantle source with or without crustal contamination (Deng, 1998; Ding et al., 2003; Guo et al., 2006). The

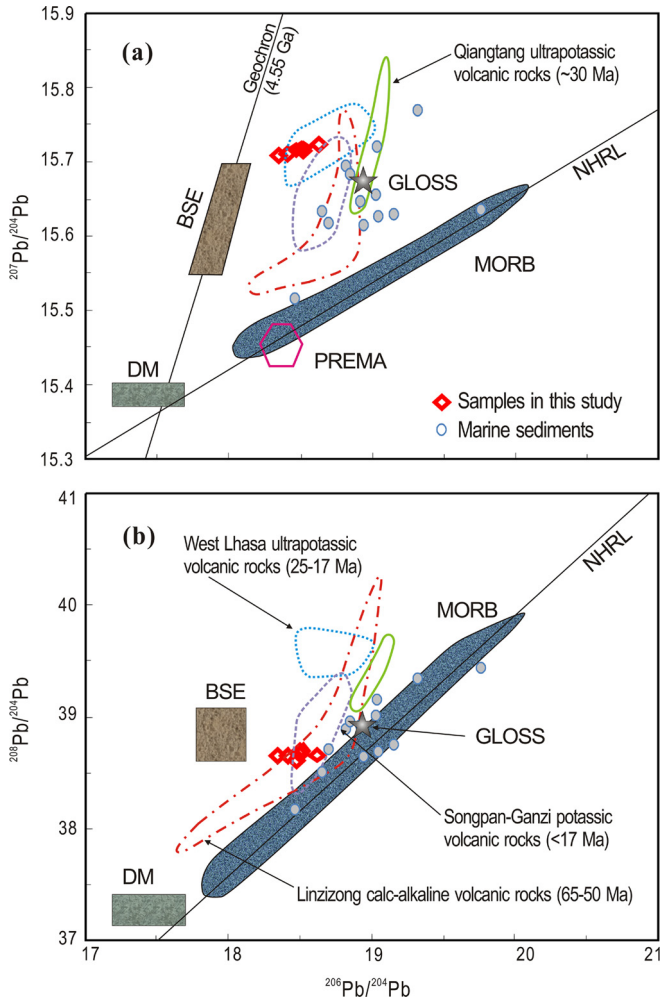

Fig. 7. (a) $^{207}Pb/^{204}Pb$ versus $^{206}Pb/^{204}Pb$ and (b) $^{208}Pb/^{204}Pb$ versus $^{206}Pb/^{204}Pb$ diagrams. The mantle sources of MORB and the mantle end-members DM, PREMA and BSE are from Zindler and Hart (1986). The fields of marine sediments and GLOSS are from Plank and Langmuir (1998). Fields for volcanic rocks from other areas in Tibet are from Ding et al. (2003).

Na-rich and calc-alkaline lavas occurring in the southern Qiangtang Terrane were also considered to have originated from a primitive mantle source (Ding et al., 2007). Although there are some crust-derived magmatic rocks present in the northern Qiangtang Terrane, most magmatic rocks are adakitic and were likely generated by partial melting of subducted sediment-dominated continental crust of the Songpan–Ganzi Terrane along the Jinshajiang suture or else originated from the interaction between mantle and sediment-derived melts derived from subducted continental crust (Lai et al., 2007; Wang et al., 2008).

With the exception of the young strongly peraluminous rhyolites exposed at the northern margin of the Songpan–Ganzi Terrane (Jolivet et al., 2003; Guo et al., 2006; Wang et al., 2012), there are no reported Cenozoic magmatic rocks derived from continental crust in the Qiangtang Terrane. The strongly peraluminous rhyolites, however, were produced by dehydration melting of metasedimentary rocks at shallow crustal depths (Wang et al., 2012). In this study, the Suyingdi rhyolites are adakitic and show geochemical characteristics of adakites derived from thickened lower crust (Fig. 10). Because of their high La/Ce and Rb/Sr ratios (Fig. 11a), these rhyolites are distinct from slab-melt derived adakites and from the Cenozoic enriched mantle-derived ultra-potassic lavas of northern Tibet. The moderate Rb/Ba and Rb/Sr ratios of the rhyolites plot along the mixing trend between basalt and the calculated psammite-derived melt (Fig. 11b), which indicates that the magma source was most likely dominated by metabasalts and clay-poor metamorphosed sedimentary rocks, such as previously subducted greywackes. This is also supported by their high Th concentrations, significantly negative Ce anomalies, and high radiogenic Pb components, which indicate strong contributions from subducted sediments (Supplementary Table 1 and Fig. 7). Therefore, we suggest that the lower crust below northern Tibet is heterogeneous and likely composed of metamorphosed mafic and sedimentary rocks. This is supported by recent studies in which mafic and felsic granulite xenoliths from the lower crust were discovered within Cenozoic potassic and ultra-potassic rocks in northern Tibet (Hacker et al., 2000; Jolivet et al., 2003; Lai et al., 2011). The geochemistry of the granulite xenoliths suggests that the protolith of the mafic granulites could have been metamorphosed from earlier underplated mafic rocks or restites from the partial melting of metamafic-intermediate rocks, whereas the felsic granulites originated from metasedimentary rocks (Lai et al., 2011).

5.3. Origin of the crustal low-velocity zones in central and northern Tibet

In the last few decades, abundant geophysical investigations have repeatedly demonstrated that there are many low-velocity zones in the middle to lower crust throughout Tibet (e.g. Nelson et al., 1996; Owens and Zandt, 1997; Wei et al., 2001; Unsworth et al., 2004; Klemperer, 2006; Caldwell et al., 2009; Bai et al., 2010; Zhang and Klemperer, 2010). The low-velocity zones were interpreted to be unusually weak layers at depths between 15 and 50 km (Unsworth et al., 2005; Le Pape et al., 2012). In southern Tibet, these weak layers are commonly considered to have formed as result of partial melting (e.g. Nelson et al., 1996; Owens and Zandt, 1997; Caldwell et al., 2009; Bai et al., 2010). Weak crustal layers have also been reported in the middle to lower crust of northern Tibet (Owens and Zandt, 1997; Wei et al., 2001; Unsworth et al., 2004; Klemperer, 2006; Le Pape et al., 2012). The granulite xenoliths discovered within the Cenozoic potassic volcanic rocks in the Qiangtang Terrane, however, record high temperatures (>800 °C) which indicate that the lower crust in central and northern Tibet may be both hot and dry (Miller et al., 1999; Hacker et al., 2000), hence they are generally considered as evidence against crustal melting in the mid- to lower crust of central and northern Tibet (Tapponnier et al., 2001; Cowgill et al., 2003). In order to interpret the crustal low-velocity zones at 15–50 km depth in central and northern Tibet, several alternative models have been suggested, including crustal shearing, preferred orientation of micas, the presence of aqueous fluids, underplating of mantle-derived melts, or the separation between an upper felsic and a lower mafic crust (Wei et al., 2001; Tapponnier et al., 2001; Vergne et al., 2002; Shapiro et al., 2004; Unsworth et al., 2004; Klemperer, 2006).

The geochemistry of the Suyingdi adakitic rhyolites indicates derivation from thickened lower crust. Zircon U–Pb dating of the rhyolites yields an eruption age of 38.2 Ma, which suggests that the lower crust of central Tibet was partially molten at least in the Eocene. This is supported by the trace element ratios of the rhyolites that show an increasing degree of partial melting in the Rb/Y–Nb/Y diagram (Fig. 12a). Their high $(La/Yb)_N$ ratios indicate that partial melting took place in the garnet stability field (Fig. 12b), which is consistent with the magma source containing both mafic and felsic granulites. The Zr saturation temperatures indicate that the Suyingdi adakitic rhyolites have partial melting temperatures between 778 °C and 797 °C (Supplementary Table 1), lower than the Zr saturation temperatures of mantle-derived (ultra-) potassic lavas in the southern Qiangtang Terrane,

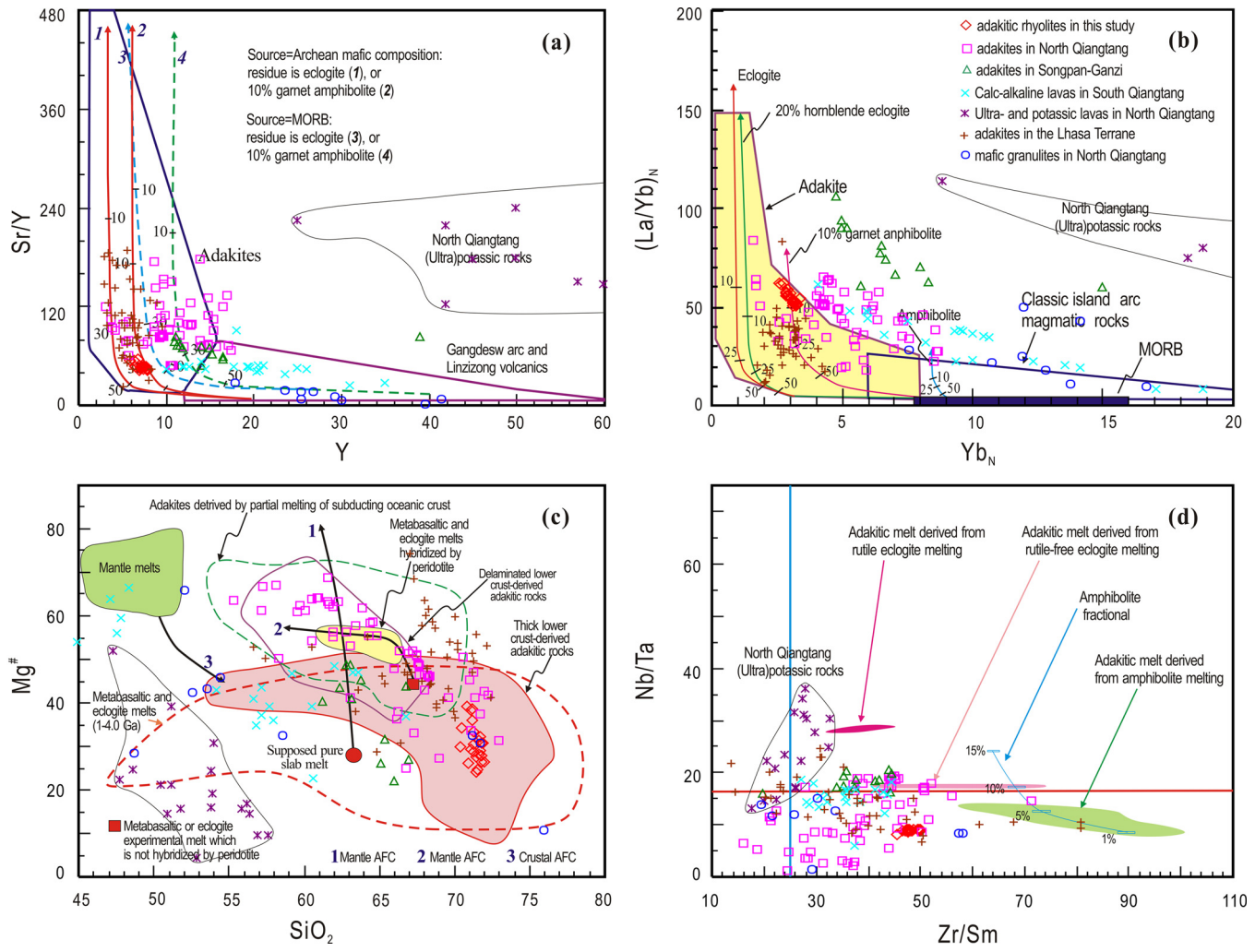

Fig. 8. (a–b) Plots of Sr/Y versus Y and $(La/Yb)_N$ versus Yb_N. Fields for adakites and classical island arc magmatic rocks are from Defant and Drummond (1990) and Martin et al. (2005). Partial melting curves for basalt residues of eclogite, garnet amphibolite and amphibolite are from Defant and Drummond (1990); (c–d) $Mg^{\#}$ versus SiO_2 and Nb/Ta versus Zr/Sm diagrams (after Martin et al., 2005). Mantle AFC curves after Stern and Kilian (1996) (curve 1) and Rapp et al. (1999) (curve 2). Crustal AFC is after Stern and Kilian (1996) (curve 3). Field of metabasaltic and eclogitic melts (dehydration melting) (1–4.0 GPa) is after Wang et al. (2007) and references therein. Fields of metabasaltic and eclogite experimental melts hybridized with peridotite are after Rapp et al. (1999). Data sources are the same as in Fig. 3.

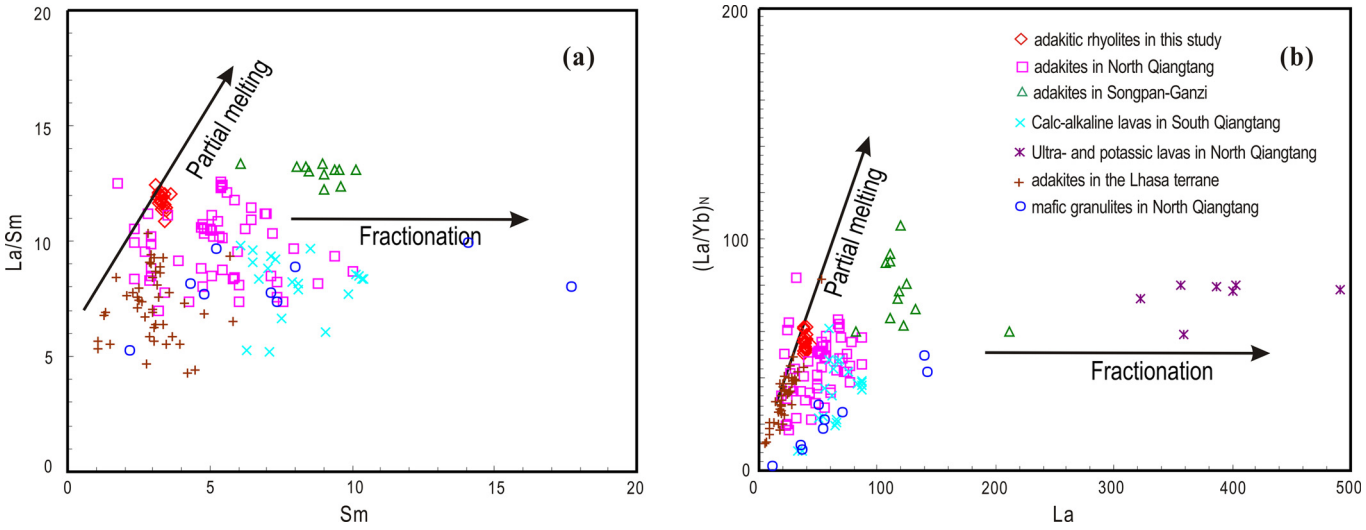

Fig. 9. Plots of (a) La/Sm versus Sm and (b) $(La/Yb)_N$ versus La, showing partial melting and fractionation trends. Data sources as in Fig. 3.

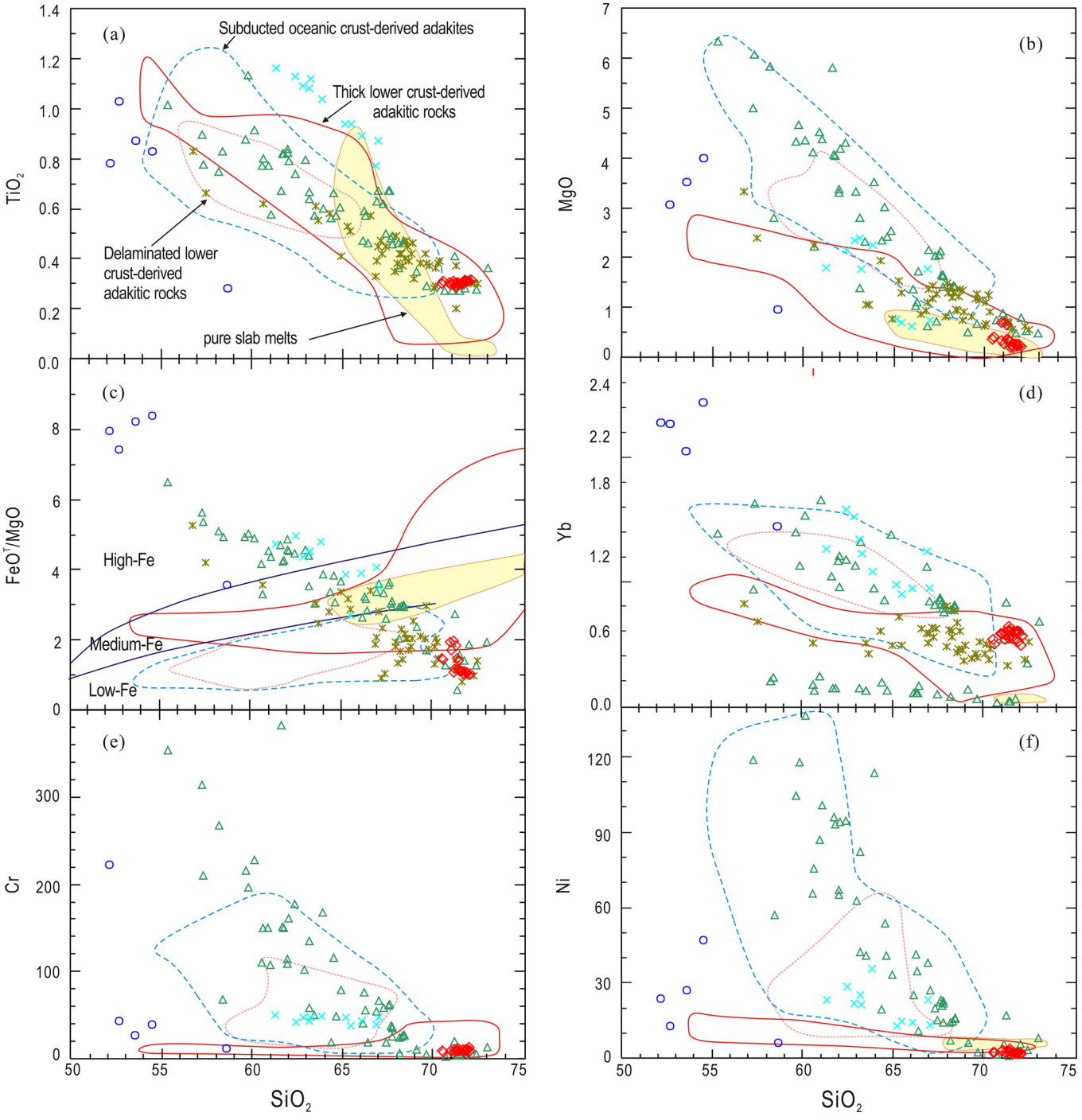

Fig. 10. Plots of selected major and trace elements versus SiO_2. Symbols are similar to those in Fig. 8.

but higher than adakites in the Lhasa Terrane (Figs. 12c–d). This suggests that partial melting was most likely triggered by the underplating of high-temperature mantle-derived magma and supports previous studies that indicate a hot lower crust beneath central and northern Tibet (Miller et al., 1999; Hacker et al., 2000). The melting temperatures of the Suyingdi rhyolites are similar to those of the high-temperature strongly peraluminous rhyolites exposed at the northern margin of the Songpan–Ganzi Terrane (Wang et al., 2012), but higher than those of the low-temperature Himalayan tourmaline leucogranites (Inger and Harris, 1993; Searle and Godin, 2003). Based on the mineral associations, Wang et al. (2012) suggested that the high-temperature, strongly peraluminous rhyolites formed by muscovite-biotite dehydration melting of metasedimentary rocks over a pressure range of 0.5–1.2 GPa, indicating a depth at 16.5–40 km. This suggests that the weak crustal layers observed in the mid- to lower crust of northern Tibet may contain partial melts, although the rhyolitic lavas have been interpreted as crustal channel flow from the Himalayan leucogranitic magmas (Wang et al., 2012). Additionally, the presence of the Hohxil K-rich adakites in the northern Songpan–Ganzi Terrane suggests that the thickened lower crust of northern Tibet was also partially molten during the Miocene (Wang et al., 2005). In combination with our data for the Suyingdi adakitic rhyolites and the previously-reported peraluminous and metaluminous adakitic

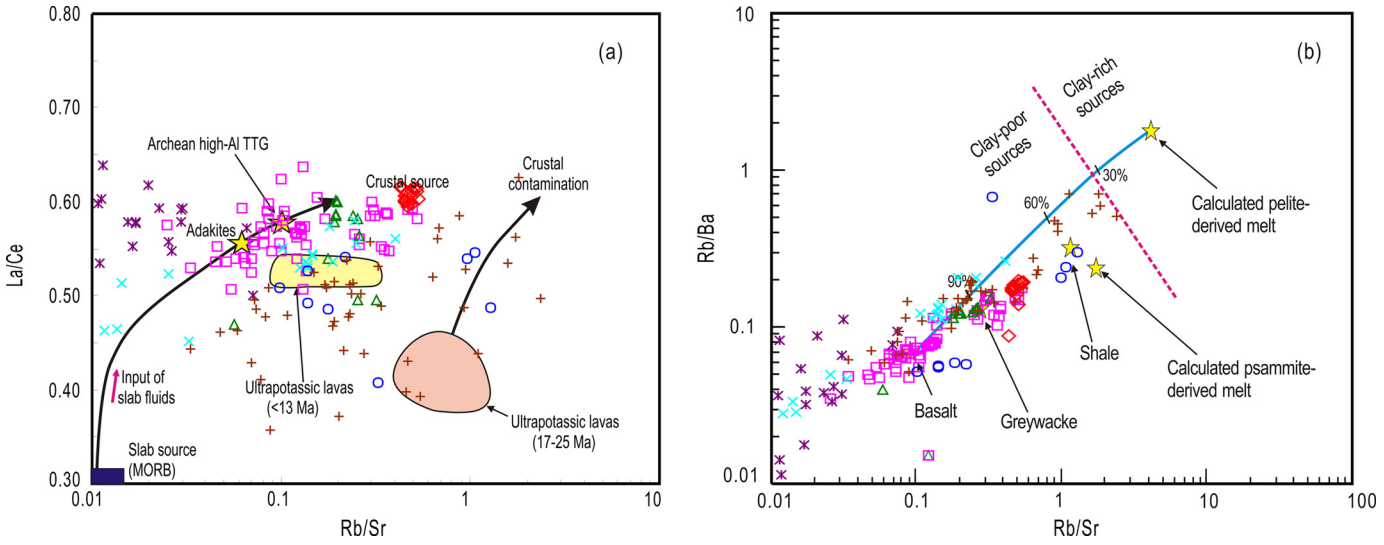

Fig. 11. Plots of (a) La/Ce versus Rb/Sr and (b) Rb/Ba versus Rb/Sr, showing geochemical compositions of magma source for the Suyingdi adakitic rhyolites. Symbols are the same as in Fig. 8. The mixing curve between the basalt- and pelite-derived melts is from Sylvester (1998).

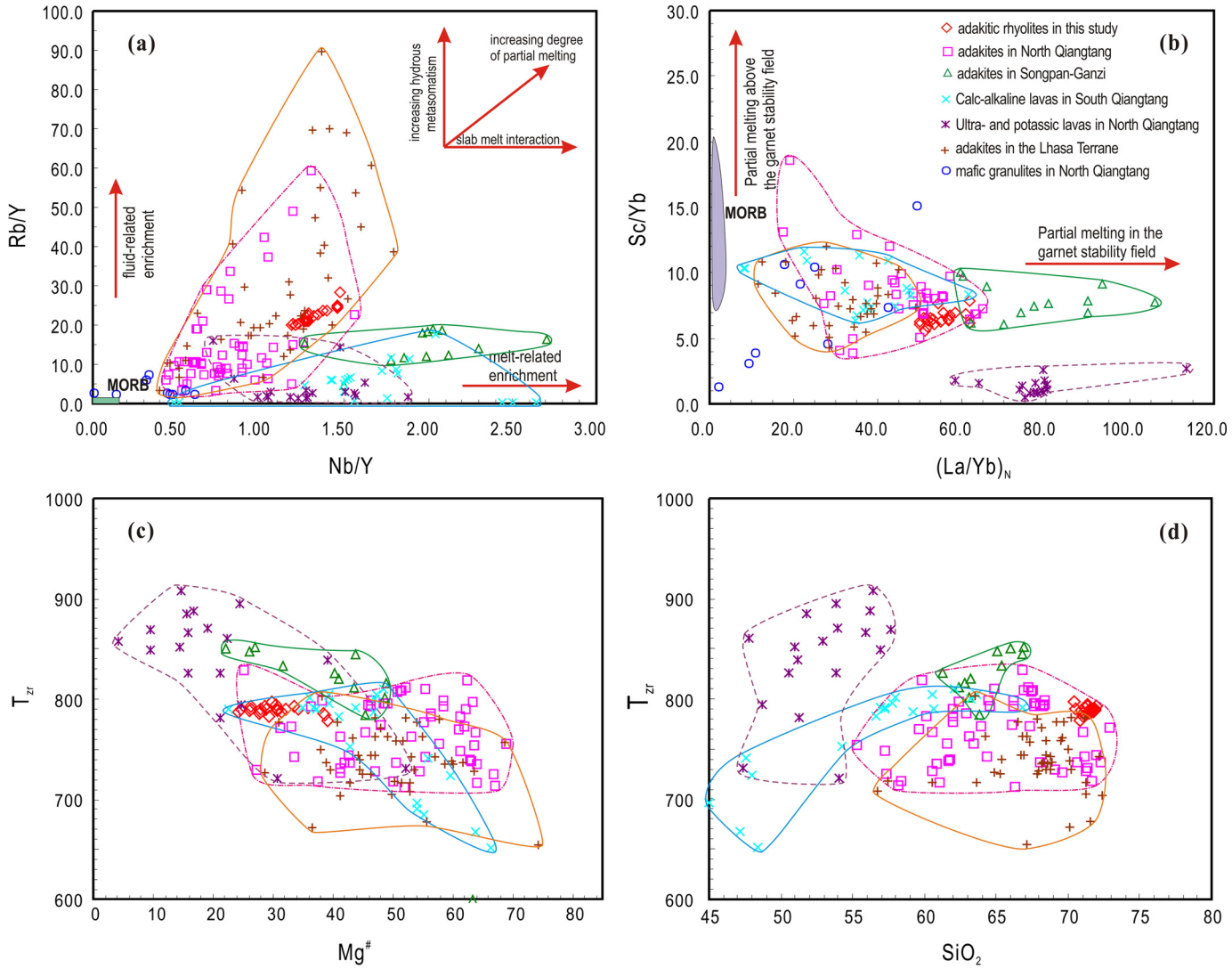

Fig. 12. Plots of (a) Rb/Y versus Nb/Y, and (b) Sc/Yb versus $(La/Yb)_N$, showing different partial melting trends for magmatic rocks; (c–d) Zr saturation temperatures versus $Mg^{\#}$ and SiO_2, respectively, for the Suyingdi adakitic rhyolites. Data sources as in Fig. 3.

rocks in the northern Qiangtang Terrane, we therefore suggest that the crustal low-velocity zones at 15–50 km depth in central and northern Tibet were most likely formed by partial melting of thickened crust in the garnet stability field.

5.4. Tectonic implications of the Cenozoic volcanic rocks in Tibet

The Eocene volcanic rocks, induced by the continent–continent collision between the Indian and Eurasian plates, record the processes of mountain building and crustal thickening, and thus are of great importance in determining the tectonic evolution of the Tibetan Plateau (Molnar et al., 1993; Rowley, 1998; Yin and Harrison, 2000). Several scenarios have been proposed to account for the formation of the Eocene volcanic rocks in central Tibet, but differ in terms of melting depth (e.g. middle to lower crust and/or lithosphere mantle) and the role of crustal deformation. The models include: 1) crustal underthrusting (Powell and Conaghan, 1975); 2) uniform thickening and shortening of the Asian lithosphere (England and Houseman, 1986; Dewey, 1988); 3) extension after the convective removal of the lower portion of the thickened Asian lithosphere (Molnar et al., 1993); and 4) extrusion along major strike-slip faults (Tapponnier et al., 1982, 2001).

The crustal underthrusting model assumes that the Tibetan Plateau is underlain by crust of double normal thickness produced by the underthrusting of the Indian continent (Powell and Conaghan, 1975). Although recent studies reveal a crustal thickness of 70–80 km in southern Tibet and 60–70 km in northern Tibet (Zhao et al., 2001; Zhang et al., 2011), the Indian continental crust has never been underthrusted as far as northern Tibet, as evidenced by the Sr–Nd isotopic data of 46–38 Ma and 18–15 Ma crustal-derived adakitic rocks (Wang et al., 2005, 2008; Lai et al., 2007). This is also supported by our Sr–Nd–Pb isotopic data of the adakitic rhyolites (Figs. 6 and 7) and mafic and felsic granulites derived from different depths of the northern Qiangtang Terrane (Lai et al., 2011), which also argue against the crustal underthrusting model.

In contrast, the thickening and shortening model suggests that the Tibetan crust was formed by horizontally northward-migrating shortening and vertical stretching of the Asian crust, and that the behavior of the lithosphere can be approximated by the modeling of a viscous sheet (Dewey and Burke, 1973). Quantitative modeling indicates that thickening and shortening should progressively spread northwards into Asia (England and Houseman, 1986). However, such a prediction is inconsistent with the distribution of Cenozoic potassic and ultra-potassic lavas (Fig. 1) that are generally attributed to rapid uplift of continental crust caused by catastrophic lithospheric convective thinning (Molnar et al., 1993; Chung et al., 1998). The published age data establish that the potassic and ultra-potassic lavas exposed in southern Tibet are much younger than those in central Tibet, but older than those in northern Tibet (Deng, 1998; Chung et al., 1998; Wang et al., 2001; Ding et al., 2003; Guo et al., 2006). Such a distribution pattern shows that the thickening of continental crust in the south, if induced by convective removal of the lower lithosphere, must have happened later than in central Tibet, but earlier than in the north. This is also inconsistent with the thickening and shortening model, which predicts crustal thickening younging northward across the whole of the Tibetan Plateau.

The extension model suggests that following convective removal of the lower part of the lithospheric mantle, it was replaced by hotter and lighter asthenosphere (England and Houseman, 1989). The model predicts a sudden increase in the surface elevation and perturbation of the geotherm, which would result in potassic and ultra-potassic lava generation via small-degree partial melting of previously enriched lithospheric mantle (Chung et al., 1998). It appears to be supported by a thin lithospheric lid observed beneath the Qiangtang and Songpan–Ganze terranes, as evidenced by geophysical investigations (Kind et al., 2002), and the anomalous seismic parameters (low Vp and Q structure) of the upper mantle that are interpreted to represent unusually high temperatures (Huang et al., 2000). This model, however, ignores the large strike-slip faults that border or slice the plateau (Tapponnier et al., 2001; Yin and Harrison, 2000). If the prediction is true, the Cenozoic potassic and ultra-potassic lavas would have formed in a short time interval accompanied with high-temperature crustal magmas and the distribution of these lavas should be distributed in a large area instead of along strike-slip faults. However, the fact is that the lavas exposed in central and northern Tibet were generated at 65–29 Ma (with a gap between 45 and 31 Ma) and $<$18 Ma, respectively (Fig. 1). In southern Tibet, the potassic and ultra-potassic lavas formed in the Miocene (26–8 Ma), and are mainly exposed in rift basins (Turner et al., 1996; Williams et al., 2004). In central Tibet, they are mostly distributed along large strike-slip faults (Yin, 2000; Tapponnier et al., 2001; Wang et al., 2001; Chung et al., 2005). The presence of high-temperature, Na-rich, and asthenospheric mantle-derived melts is one of the diagnostic features of the extension model. However, such melts occur only rarely in the eastern Qiangtang Terrane and its southern margin (Wang et al., 2001; Ding et al., 2003, 2007), whereas none are documented elsewhere in central and northern Tibet. Therefore, the diachronous distribution of Cenozoic magmatism in Tibet is inconsistent with a simple extension model.

The extrusion model emphasizes the significant slip that took place along several major strike-slip faults to facilitate eastward extrusion of crustal material (Molnar and Tapponnier, 1975; Tapponnier et al., 1982). It suggests that uplift of the plateau occurred in three steps induced by oblique subduction of Asian lithospheric mantle, accompanied by extrusion and crustal thickening (Tapponnier et al., 2001). Although this model is consistent with studies of crustal deformation and can explain the north-south trending rifts (Yin and Harrison, 2000) and the diachronous nature of Cenozoic potassic and ultra-potassic lavas in Tibet (Tapponnier et al., 2001; Wang et al., 2001), it does not explain the low-velocity zones in the middle to lower crust as defined by geophysical data (Wei et al., 2001; Bai et al., 2010).

The low-velocity zones are considered to be the result of partial melting, suggesting that the weak middle or lower crust can flow on geologic time scales (Bird, 1991; Royden et al., 1997; Clark and Royden, 2000). This is referred to as channel flow and extends from the center to the edge of the plateau, and most likely including the east–west extrusion of the plateau (Royden et al., 2008; Bai et al., 2010). However, whether the formation of the low-velocity zones can be attributed to the oblique subduction of Asian lithosphere or to other tectonic scenarios is poorly constrained. The Suyingdi adakitic rhyolites, as discussed above, were produced by partial melting of thickened lower crust, indicating that the low-velocity zones beneath central Tibet were most likely formed by partial melting. Their high Th concentrations, significantly negative Ce anomalies, and moderate Rb/Ba and Rb/Sr ratios show significant contributions from subducted sediments. Because the Sr–Nd isotopic compositions of the rhyolites overlap the fields of Triassic Songpan–Ganzi flysch (Fig. 6; She et al., 2006) and the Pb isotopic compositions are similar to those of marine sediments (Fig. 7; Plank and Langmuir, 1998), we suggest that subducted sedimentary rocks in the magmatic source were formed by the southward subduction of the Songpan–Ganzi Terrane. This is supported by recent crustal xenolith studies that reveal the lower crust beneath northern Qiangtang mainly consists of Triassic Songpan–Ganzi sedimentary rocks subducted in the Early Mesozoic or Cenozoic (Hacker et al., 2000; Kapp et al., 2003). Therefore, our study indicates that the forma-

tion of the low-velocity zones in central Tibet was most likely induced by the oblique subduction of Asian lithosphere, which in turn favors the extrusion model.

6. Conclusions

(1) The Suyingdi rhyolites erupted at 38.2 Ma and show geochemical characteristics of adakitic rocks.
(2) These adakitic rhyolites were most likely produced by partial melting of a thickened lower crust that consists of granulite facies rocks.
(3) The magma source of the adakitic rhyolites was probably a mixture of metamorphosed mafic and sedimentary rocks, which suggests that the lower crust of central Tibet is heterogeneous.
(4) The low-velocity zones in the mid- to lower crust of central and northern Tibet were most likely generated by crustal melting.

Acknowledgements

We are very grateful to An Yin for efficient editorial handling. Our paper has benefited from the constructive suggestions and comments of Haibo Zou, which have greatly improved the manuscript. This study was supported by the "Strategic Priority Research Program (B)" of the Chinese Academy of Sciences (XDB03010600), the GIGCAS 135 project of the Guangzhou Institute of Geochemistry (Y234021001) and a grant from the State Key Laboratory of Isotope Geochemistry (SKLIG-RC-12-01). This is contribution No. IS-2020 of GIGCAS and The Institute for Geoscience (TIGeR) publication number 608.

Appendix A. Supplementary material

Supplementary material related to this article can be found online at http://dx.doi.org/10.1016/j.epsl.2015.01.007.

References

Ahmad, T., Harris, N., Bickle, M., Chapman, H., Bunbury, J., Prince, C., 2000. Isotopic constraints on the structural relationships between the Lesser Himalayan Series and the High Himalayan Crystalline Series, Garhwal Himalaya. Geol. Soc. Am. Bull. 112, 467–477.
Arnaud, N.O., Vidal, P., Tapponnier, P., Matte, P., Deng, W.M., 1992. The high K_2O volcanism of northwestern Tibet: geochemistry and tectonic implications. Earth Planet. Sci. Lett. 111, 351–367.
Atherton, M.P., Petford, N., 1993. Generation of sodium rich magmas from newly underplated basaltic crust. Nature 362, 144–146.
Bai, D., Unsworth, M.J., Meju, M.A., Ma, X., Teng, J., Kong, X., Sun, Y., Sun, J., Wang, L., Jiang, C., Zhao, C., Xiao, P., Liu, M., 2010. Crustal deformation of the eastern Tibetan plateau revealed by magnetotelluric imaging. Nat. Geosci.l 3, 358–362.
Bird, P., 1991. Lateral extrusion of lower crust from under high topography in the isostatic limit. J. Geophys. Res. 96, 10275–10286.
Blisniuk, P.M., Hacker, B.R., Glodny, J., Ratschbacher, L., Bi, S., Wu, Z., McWilliams, M.O., Calvert, A., 2001. Normal faulting in central Tibet since at least 13.5 Myr ago. Nature 412 (6847), 628–632.
Bruguier, O., Lancelot, J.R., Malavieille, J., 1997. U–Pb dating on single detrital zircon grains from the Triassic Songpan–Ganzi flysch (central China): provenance and tectonic correlations. Earth Planet. Sci. Lett. 152, 217–231.
Caldwell, B., Klemperer, S.L., Rai, S.S., Lawrence, J.F., 2009. Partial melt in the upper–middle crust of the northwest Himalaya revealed by Rayleigh wave dispersion. Tectonophysics 477, 58–65.
Castillo, P.R., Janney, P.E., Solidum, R.U., 1999. Petrology and geochemistry of Camiguin island, southern Philippines: insights to the source of adakites and other lavas in a complex arc setting. Contrib. Mineral. Petrol. 134, 33–51.
Chemenda, A.I., Burg, J.P., Mattauer, M., 2000. Evolutionary model of the Himalaya–Tibet system: geopoem based on new modelling, geological and geophysical data. Earth Planet. Sci. Lett. 174, 397–409.
Chen, J.L., Xu, J.F., Wang, B.D., Kang, Z.Q., Jie, L., 2010. Origin of Cenozoic alkaline potassic volcanic rocks at KonglongXiang, Lhasa terrane, Tibetan Plateau: products of partial melting of a mafic lower-crustal source? Chem. Geol. 273, 286–299.
Chung, S.-L., Lo, C.-H., Lee, T.-Y., Zhang, Y., Xie, Y., Li, X., Wang, K.-L., Wang, P.-L., 1998. Diachronous uplift of the Tibetan Plateau starting 40 Myr ago. Nature 394, 769–773.
Chung, S.-L., Liu, D.-Y., Ji, J.-Q., Chu, M.-F., Lee, H.-Y., Wen, D.-J., Lo, C.-H., Lee, T.-Y., Qian, Q., Zhang, Q., 2003. Adakites from continental collision zones: melting of thickened lower crust beneath southern Tibet. Geology 31, 1021–1024.
Chung, S.-L., Chu, M.-F., Zhang, Y., Xie, Y., Lo, C.-H., Lee, T.-Y., Lan, C.-Y., Li, X., Zhang, Q., Wang, Y., 2005. Tibetan tectonic evolution inferred from spatial and temporal variations in post-collisional magmatism. Earth-Sci. Rev. 68, 173–196.
Clark, M.K., Royden, L.H., 2000. Topographic ooze: building the eastern margin of Tibet by lower crustal flow. Geology 28, 703–706.
Coleman, M.E., Hodges, K.V., 1995. Evidence for Tibetan plateau uplift before 14 Myr ago from a new minimum estimate for east–west extension. Nature 374, 49–52.
Condie, K.C., 2005. TTGs and adakites: are they both slab melts? Lithos 80 (1–4), 33–44.
Cooper, K.M., Reid, M.R., Dunbar, N.W., McIntosh, W.C., 2002. Origin of mafic magmas beneath northwestern Tibet: constraints from ^{230}Th–^{238}U disequilibria. Geochem. Geophys. Geosyst. 3 (11), 1065. http://dx.doi.org/10.1029/2002GC000332.
Coulon, C., Maluski, H., Bollinger, C., Wang, S., 1986. Mesozoic and Cenozoic volcanic rocks from central and southern Tibet: $^{40}Ar/^{39}Ar$ dating, petrological characteristics and geodynamic significance. Earth Planet. Sci. Lett. 79, 281–302.
Cowgill, E., Yin, A., Harrison, T.M., Wang, X.-F., 2003. Reconstruction of the Altyn Tagh fault based on U–Pb geochronology: role of back thrusts, mantle sutures, and heterogeneous crustal strength in forming the Tibetan Plateau. J. Geophys. Res. 108, 2346. http://dx.doi.org/10.1029/2002JB002080.
Davies, J.H., von Blanckenburg, F., 1995. Slab breakoff: a model of lithosphere detachment and its test in the magmatism and deformation of collisional orogens. Earth Planet. Sci. Lett. 129, 85–102.
Debon, F., Le Fort, P., Sheppard, S.M.F., Sonet, J., 1986. The four plutonic belts of the trans-Himalaya–Himalaya: a chemical, mineralogical, isotopic and chronological synthesis along a Tibet–Nepal section. J. Petrol. 27, 219–250.
DeCelles, P.G., Robinson, D.M., Zandt, G., 2002. Implications of shortening in the Himalayan fold-thrust belt for uplift of the Tibetan plateau. Tectonics 21 (6), 1062. http://dx.doi.org/10.1029/2001TC001322.
Defant, M.J., Drummond, M.S., 1990. Derivation of some modern arc magmas by melting of young subducted lithosphere. Nature 347, 662–665.
Deng, W., 1998. Cenozoic Intraplate Volcanic Rocks in the Northern Qinghai–Xizang (Tibetan) Plateau. Geological Publishing House, Beijing, 180 pp.
Dewey, J.F., 1988. Extensional collapse of orogens. Tectonics 7, 1123–1139.
Dewey, J.F., Burke, K., 1973. Tibetan, Variscan and Precambrian basement reactivation: products of a continental collision. J. Geol. 81, 683–692.
Ding, L., Kapp, P., Zhong, D., Deng, W., 2003. Cenozoic volcanism in Tibet: evidence for a transition from oceanic to continental subduction. J. Petrol. 44, 1833–1865.
Ding, L., Kapp, P., Wan, X., 2005. Paleocene–Eocene record of ophiolite obduction and initial India–Asia collision, south central Tibet. Tectonics 24, TC3001. http://dx.doi.org/10.1029/2004TC001729.
Ding, L., Kapp, P., Yue, Y.H., Lai, Q.Z., 2007. Postcollisional calc-alkaline lavas and xenoliths from the southern Qiangtang terrane, central Tibet. Earth Planet. Sci. Lett. 254, 28–38.
Dupont-Nivet, G., Krijgsman, W., Langereis, C.G., Abels, H.A., Dai, S., Fang, X., 2007. Tibetan Plateau aridification linked to global cooling at the Eocene–Oligocene transition. Nature 445 (7128), 635–638.
England, P., Houseman, G., 1986. Finite strain calculations of continental deformation. Comparison with the India–Asia collision zone. J. Geophys. Res. 91, 3664–3676. http://dx.doi.org/10.1029/JB091iB03p03664.
England, P., Houseman, G., 1989. Extension during continental convergence with application to the Tibetan Plateau. J. Geophys. Res. 94, 17561–17579.
Gao, Y.F., Hou, Z.Q., Kamber, B.S., Wei, R., Meng, X., Zhao, R., 2007. Adakite-like porphyries from the southern Tibetan continental collision zones: evidence for slab melt metasomatism. Contrib. Mineral. Petrol. 153, 105–120.
Gao, Y.F., Wei, R.H., Hou, Z.Q., Tian, S.H., Zhao, R.S., 2008. Eocene high-MgO volcanism in southern Tibet: new constraints for mantle source characteristics and deep processes. Lithos 105, 63–72.
Gao, Y.F., Yang, Z.S., Hou, Z.Q., Wei, R.H., Meng, X.J., Tian, S.H., 2010. Eocene potassic and ultrapotassic volcanism in south Tibet: new constraints on mantle source characteristics and geodynamic processes. Lithos 117, 20–32.
Guo, Z.F., Wilson, M., Liu, J., Mao, Q., 2006. Post-collisional, potassic and ultrapotassic magmatism of the Northern Tibetan Plateau: constraints on the characteristics of the mantle source, geodynamic setting and uplift mechanisms. J. Petrol. 47 (6), 1177–1220.
Guo, Z.F., Wilson, M., Liu, J.Q., 2007. Post-collisional adakites in south Tibet: products of partial melting of subduction-modified lower crust. Lithos 96, 205–224.
Guo, Z.F., Wilson, M., Zhang, M.L., Cheng, Z.H., Zhang, L.H., 2013. Post-collisional, K-rich mafic magmatism in south Tibet: constraints on Indian slab-to-wedge transport processes and plateau uplift. Contrib. Mineral. Petrol. 165, 1311–1340.
Hacker, B.R., Gnos, E., Ratschbacher, L., Grove, M., McWilliams, M., Wan, J., 2000. Hot and dry xenoliths from the bottom of Tibet. Science 287, 2463–2466.
Harris, N., 2006. The elevation history of the Tibetan Plateau and its implications for the Asian monsoon. Palaeogeogr. Palaeoclimatol. Palaeoecol. 241 (1), 4–15.

Harris, N.B.W., Xu, R.-H., Lewis, C.L., Jin, C.-W., 1988. Plutonic rocks of the 1985 Tibet Geotraverse: Lhasa to Golmud. Philos. Trans. R. Soc. Lond. A 327, 145–168.
Harrison, T.M., Lovera, O.M., Grove, M., 1997. New insights into the origin of two contrasting Himalayan granite belts. Geology 25, 899–902.
Holbig, E.S., Grove, T.L., 2008. Mantle melting beneath the Tibetan Plateau: experimental constraints on the ultrapotassic magmatism. J. Geophys. Res. 113, B04210. http://dx.doi.org/10.1029/2007JB005149.
Hou, Z.Q., Gao, Y.F., Qu, X.M., Rui, Z.Y., Mo, X.X., 2004. Origin of adakitic intrusives generated during mid-Miocene east–west extension in southern Tibet. Earth Planet. Sci. Lett. 220, 139–155.
Huang, W.-C., Ni, J.F., Tilmann, F., Nelson, D., Guo, J., Zhao, W., Mechie, J., Kind, R., Saul, J., Rapine, R., Hearn, T.M., 2000. Seismic polarization anisotropy beneath the central Tibetan plateau. J. Geophys. Res. 105, 27979–27989.
Inger, S., Harris, N., 1993. Geochemical constraints on leucogranite magmatism in the Langtang Valley, Nepal Himalaya. J. Petrol. 34 (2), 345–368.
Ji, W.Q., Wu, F.Y., Chung, S.L., Li, J.X., Liu, C.Z., 2009. Zircon U–Pb geochronology and Hf isotopic constraints on petrogenesis of the Gangdese batholith, southern Tibet. Chem. Geol. 262, 229–245.
Jolivet, M., Brunel, M., Seward, D., Xu, Z., Yang, J., Malavieille, J., Roger, F., Leyreloup, A., Arnaud, N., Wu, C., 2003. Neogene extension and volcanism in the Kunlun Fault Zone, northern Tibet: new constraints on the age of the Kunlun Fault. Tectonics 22, 1052. http://dx.doi.org/10.1029/2002TC001428.
Kapp, P., Yin, A., Manning, C., Murphy, M.A., Harrison, T.M., Spurlin, M., Ding, L., Deng, X.-G., Wu, C.-M., 2000. Blueschist-bearing metamorphic core complexes in the Qiangtang block reveal deep crustal structure of northern Tibet. Geology 28, 19–22.
Kapp, P., Murphy, M.A., Yin, A., Harrison, T.M., Ding, L., Guo, J., 2003. Mesozoic and Cenozoic tectonic evolution of the Shiquanhe area of western Tibet. Tectonics 22 (4), 1043. http://dx.doi.org/10.1029/2002TC001383.
Kay, R.W., Kay, S.M., 1993. Delamination and delamination magmatism. Tectonophysics 219, 177–189.
Kind, R., Yuan, X., Saul, J., Nelson, D., Sobolev, S.V., Mechie, J., Zhao, W., Kosarev, G., Ni, J., Achauer, U., Jiang, M., 2002. Seismic images of crust and upper mantle beneath Tibet: evidence for Eurasian plate subduction. Science 298, 1219–1221.
Klemperer, S.L., 2006. Crustal flow in Tibet: geophysical evidence for the physical state of Tibetan lithosphere, and inferred patterns of active flow. In: Law, R.D., Searle, M.P., Godin, L. (Eds.), Channel Flow, Ductile Extrusion and Exhumation in Continental Collision Zones. In: Geological Society of London, Special Publications, vol. 268, pp. 39–70.
Lai, S.C., Qin, J.F., Li, Y.F., 2007. Partial melting of thickened Tibetan crust: geochemical evidence from Cenozoic adakitic volcanic rocks. Int. Geol. Rev. 49, 357–373.
Lai, S.C., Qin, J.F., Grapes, R., 2011. Petrochemistry of granulite xenoliths from the Cenozoic Qiangtang volcanic field, northern Tibetan Plateau: implications for lower crust composition and genesis of the volcanism. Int. Geol. Rev. 53, 926–945.
Le Pape, F., Jones, A.G., Vozar, J., Wenbo, W., 2012. Penetration of crustal melt beyond the Kunlun Fault into northern Tibet. Nat. Geosci. 5, 330–335.
Li, C., Cheng, L.R., Hu, K., Yang, Z.R., Hong, Y.R., 1995. Study on the Paleo–Tethys Suture Zone of Lungmu Co–Shuanghu, Tibet. Geological Publishing House, Beijing, pp. 1–131 (in Chinese with English abstract).
Macpherson, C.G., Dreher, S.T., Thirlwall, M.F., 2006. Adakites without slab melting: high pressure differentiation of island arc magma, Mindanao, the Philippines. Earth Planet. Sci. Lett. 243 (3–4), 581–593.
Martin, H., Smithies, R.H., Rapp, R., Moyen, J.F., Champion, D., 2005. An overview of adakite, tonalite-trondhjemite-granodiorite (TTG), and sanukitoid: relationships and some implications for crustal evolution. Lithos 79, 1–24.
McKenna, L.W., Walker, J.D., 1990. Geochemistry of crustally derived leucocratic igneous rocks from the Ulugh Muztagh area, northern Tibet, and their implications for the formation of the Tibetan Plateau. J. Geophys. Res. 95, 21,483–21,502.
Miller, C., Schuster, R., Klotzli, U., Frank, W., Grasemann, B., 1999. Post-collisional potassic and ultra-potassic magmatism in SW Tibet: geochemical and Sr–Nd–Pb–O isotopic constraints for mantle source characteristics and petrogenesis. J. Petrol. 83, 5361–5375.
Miller, C., Schuster, R., Klötzli, U., Frank, W., Grasemann, B., 2000. Late Cretaceous–Tertiary magmatic and tectonic events in the Transhimalaya batholith (Kailas area, SW Tibet). Schweiz. Mineral. Petrogr. Mitt. 80, 1–20.
Miller, C., Thöni, M., Frank, W., Schuster, R., Melcher, F., Meisel, T., Zanetti, A., 2003. Geochemistry and tectonomagmatic affinity of the Yungbwa ophiolite, SW Tibet. Lithos 66, 155–172.
Mo, X.X., Dong, G.C., Zhao, Z.D., Zhou, S., Wang, L.L., Qiu, R.Z., Zhang, F.Q., 2005. Spatial and temporal distribution and characteristics of granitoids in the Gangdese, Tibet, and implications for crustal growth and evolution. Geol. J. China Univ. 11 (3), 281–290 (in Chinese with an English abstract).
Mo, X.X., Hou, Z.Q., Niu, Y.L., Dong, G.C., Qu, X.M., Zhao, Z.D., Yang, Z.M., 2007. Mantle contributions to crustal thickening during continental collision: evidence from Cenozoic igneous rocks in southern Tibet. Lithos 96, 225–242.
Mo, X.X., Niu, Y.L., Dong, G.C., Zhao, Z.D., Hou, Z.Q., Su, Z., Ke, S., 2008. Contribution of syncollisional felsic magmatism to continental crust growth: a case study of the Paleogene Linzizong volcanic succession in southern Tibet. Chem. Geol. 250, 49–67.
Molnar, P., Tapponnier, P., 1975. Cenozoic tectonics of Asia: effects of a continental collision. Science 189, 419–426.
Molnar, P., England, P., Martinod, J., 1993. Mantle dynamics, the uplift of the Tibetan plateau, and the Indian monsoon. Rev. Geophys. 31, 357–396.
Murphy, M.A., Yin, A., Harrison, T.M., Dürr, S.B., Chen, Z., Ryerson, F.J., Kidd, W.S.F., Wang, X., Zhou, X., 1997. Did the Indo–Asian collision along create the Tibetan plateau? Geology 25, 719–722.
Nábělek, J., Hetényi, G., Vergne, J., Sapkota, S., Kafle, B., Jiang, M., Su, H., Chen, J., Huang, B.-S., the Hi-CLIMB Team, 2009. Underplating in the Himalaya–Tibet collision zone revealed by the Hi-CLIMB experiment. Science 325, 1371–1374.
Nelson, K.D., Zhao, W.J., Brown, L.D., Kuo, J., Che, J., et al., 1996. Partially molten middle crust beneath southern Tibet: synthesis of project INDEPTH results. Science 274, 1684–1688.
Owens, T.J., Zandt, G., 1997. Implications of crustal property variations for models of Tibetan plateau evolution. Nature 387, 37–43.
Plank, T., Langmuir, C.H., 1998. The chemical composition of subducting sediment and its consequences for the crust and mantle. Chem. Geol. 145, 325–394.
Powell, C.M., Conaghan, P.J., 1975. Tectonic models of the Tibetan Plateau. Geology 3, 727–731.
Prouteau, G., Scaillet, B., 2003. Experimental constraints on the origin of the Pinatubo dacite. J. Petrol. 44 (12), 2203–2241.
Qu, X.M., Hou, Z.Q., Li, Y.G., 2004. Melt components derived from a subducted slab in late orogenic ore-bearing porphyries in the Gangdese copper belt, southern Tibetan plateau. Lithos 74, 131–148.
Rapp, R.P., Shimizu, N., Norman, M.D., Applegate, G.S., 1999. Reaction between slab-derived melts and peridotite in the mantle wedge: experimental constraints at 3.8 GPa. Chem. Geol. 160, 335–356.
Raymo, M.E., Ruddiman, W.F., 1992. Tectonic forcing of Late Cenozoic climate. Nature 359, 117–122.
Roger, F., Tapponnier, P., Arnaud, N., Schärer, U., Brunel, M., Xu, Z., Yang, J., 2000. An Eocene magmatic belt across central Tibet: mantle subduction triggered by the Indian collision? Terra Nova 12, 102–108.
Royden, L.H., Burchfiel, B.C., King, R.W., Wang, E., Chen, Z., Shen, F., Liu, Y., 1997. Surface deformation and lower crust flow in Eastern Tibet. Science 276, 788–790.
Royden, L.H., Burchfiel, B.C., Van Der Hilst, R.D., 2008. The geological evolution of the Tibetan Plateau. Science 321, 1054–1058.
Rowley, D.B., 1998. Minimum age of initiation of collision between India and Asia north of Everest based on the subsidence history of the Zhepure mountain section. J. Geol. 106, 229–235.
Ruddiman, W., 1998. Early uplift in Tibet? Nature 394, 723–725.
Searle, M.P., Godin, L., 2003. The South Tibetan Detachment and the Manaslu leucogranite: a structural reinterpretation and restoration of the Annapurna–Manaslu Himalaya, Nepal. J. Geol. 111, 505–523.
Sengör, A.M.C., 1984. The Cimmeride orogenic system and the tectonics of Eurasia. Spec. Pap., Geol. Soc. Am. 195, 88 pp.
Shapiro, N.M., Ritzwoller, M.H., Molnar, P., Levin, V., 2004. Thinning and flow of Tibetan crust constrained by seismic anisotropy. Science 305, 233–236.
She, Z.B., Ma, C.Q., Mason, R., Li, J.W., Wang, G.C., Lei, Y.H., 2006. Provenance of the Triassic Songpan–Ganzi flysch, west China. Chem. Geol. 231, 159–175.
Smithies, R.H., 2000. The Archaean tonalite–trondhjemite–granodiorite (TTG) series is not an analogue of Cenozoic adakite. Earth Planet. Sci. Lett. 182, 115–125.
Spurlin, M.S., Yin, A., Horton, B.K., Zhou, J., Wang, J., 2005. Structural evolution of the Yushu-Nangqian region and its relationship to syncollisional igneous activity, east central Tibet. Geol. Soc. Am. Bull. 117, 1293–1317.
Stern, C.R., Kilian, R., 1996. Role of the subducted slab, mantle wedge and continental crust in the generation of adakites from the Austral Volcanic Zone. Contrib. Mineral. Petrol. 123, 263–281.
Streck, M.J., Leeman, W.P., Chesley, J., 2007. High-magnesian andesite from Mount Shasta: a product of magma mixing and contamination, not a primitive mantle melt. Geology 35 (4), 351–354.
Sun, S.S., McDonough, W.F., 1989. Chemical and isotopic systematics of oceanic basalts: implications for mantle composition and processes. In: Saunders, A.D., Norry, M.J. (Eds.), Magmatism in Ocean Basins. In: Geological Society of London, Special Publications, vol. 42, pp. 313–345.
Sylvester, P.J., 1998. Postcollisional strongly peraluminous granites. Lithos 45, 29–44.
Tapponnier, P., Peltzer, G., Ledain, A.Y., Armijo, R., Cobbold, P.R., 1982. Propagating extrusion tectonics in Asia: new insights from simple experiments with plasticine. Geology 10, 611–616.
Tapponnier, P., Zhiqin, X., Roger, F., Meyer, B., Arnaud, N., Wittlinger, G., Jingsui, Y., 2001. Oblique stepwise rise and growth of the Tibet plateau. Science 294 (5547), 1671–1677.
Turner, S., Hawkesworth, C.J., Liu, J., Rogers, N., Kelley, S., van Calsteren, P., 1993. Timing of Tibetan uplift constrained by analysis of volcanic rocks. Nature 364, 50–54.
Turner, S., Arnaud, N., Liu, J., Rogers, N., Hawkesworth, C., Harris, N., Kelley, S., Van Calsteren, P., Deng, W., 1996. Post-collision, shoshonitic volcanism on the Tibetan Plateau: implications for convective thinning of the lithosphere and the source of ocean island basalts. J. Petrol. 37 (1), 45–71.
Unsworth, M., Wei, W., Jones, A.G., Li, S., Bedrosian, P., Booker, J., Jin, S., Deng, M., Tan, H., 2004. Crustal and upper mantle structure of northern Tibet imaged with magnetotelluric data. J. Geophys. Res. 109, B02403. http://dx.doi.org/10.1029/2002JB002305.

Unsworth, M.J., Jones, A.G., Wei, W., Marquis, G., Gokarn, S.G., Spratt, J.E., 2005. Crustal rheology of the Himalaya and Southern Tibet inferred from magnetotelluric data. Nature 438, 78–81.

Vergne, J., Wittlinger, G., Hui, Q., Tapponnier, P., Poupinet, G., Mei, J., Herquel, G., Paul, A., 2002. Seismic evidence for stepwise thickening of the crust across the NE Tibetan plateau. Earth Planet. Sci. Lett. 203, 25–33.

Wang, J.H., Yin, A., Harrison, T.M., Grove, M., Zhang, Y.Q., Xie, G.H., 2001. A tectonic model for Cenozoic igneous activities in the eastern Indo-Asian collision zone. Earth Planet. Sci. Lett. 188, 123–133.

Wang, Q., McDermott, F., Xu, J.F., Bellon, H., Zhu, Y.T., 2005. Cenozoic K-rich adakitic volcanic rocks in the Hohxil area, northern Tibet: lower-crustal melting in an intracontinental setting. Geology 33, 465–468.

Wang, Q., Xu, J.F., Jian, P., Bao, Z.W., Zhao, Z.H., Li, C.F., Xiong, X.L., Ma, J.L., 2006. Petrogenesis of adakitic porphyries in an extensional tectonic setting, Dexing, South China: implications for the genesis of porphyry copper mineralization. J. Petrol. 47, 119–144.

Wang, Q., Wyman, D.A., Xu, J., Jian, P., Zhao, Z., Li, C., Xu, W., Ma, J., He, B., 2007. Early Cretaceous adakitic granites in the Northern Dabie Complex, central China: implications for partial melting and delamination of thickened lower crust. Geochim. Cosmochim. Acta 71 (10), 2609–2636.

Wang, Q., Wyman, D.A., Xu, J., Dong, Y., Vasconcelos, P.M., Pearson, N., Wan, Y., Dong, H., Li, C., Yu, Y., Zhu, T., Feng, X., Zhang, Q., Zi, F., Chu, Z., 2008. Eocene melting of subducting continental crust and early uplifting of central Tibet: evidence from central-western Qiangtang high-K calc-alkaline andesites, dacites and rhyolites. Earth Planet. Sci. Lett. 272, 158–171.

Wang, Q., Chung, S.L., Li, X.H., Wyman, D., Li, Z.X., Sun, W.D., Qiu, H.N., Liu, Y.S., Zhu, Y.T., 2012. Crustal melting and flow beneath Northern Tibet: evidence from mid-miocene to quaternary strongly peraluminous rhyolites in the southern Kunlun range. J. Petrol. 53, 2523–2566.

Wei, W.B., Unsworth, M., Jones, A., Booker, J., Tan, H.D., Nelson, D., Chen, L.S., Li, S.H., Solon, K., Bedrosian, P., Jin, S., Deng, M., Ledo, J., Ray, D., Roberts, B., 2001. Detection of widespread fluids in the Tibetan crust by magnetotelluric studies. Science 292, 716–718.

Wen, D.R., Liu, D.Y., Chung, S.L., Chu, M.F., Ji, J.Q., Zhang, Q., Song, B., Lee, T.Y., Yeh, M.W., Lo, C.H., 2008. Zircon SHRIMP U–Pb ages of the Gangdese Batholith and implications for Neotethyan subduction in southern Tibet. Chem. Geol. 252, 191–201.

Williams, H., Turner, S., Kelley, S., Harris, N., 2001. Age and composition of dikes in southern Tibet: new constraints on the timing of east–west extension and its relationship to post-collisional volcanism. Geology 29, 339–342.

Williams, H., Turner, S., Pearce, J.A., Kelley, S.P., Harris, N.B.W., 2004. Nature of the source regions for post-collisional, potassic magmatism in southern and northern Tibet from geochemical variations and inverse trace element modelling. J. Petrol. 45, 555–607.

Xu, J.F., Shinjio, R., Defant, M.J., Wang, Q., Rapp, R.P., 2002. Origin of Mesozoic adakitic intrusive rocks in the Ningzhen area of east China: partial melting of delaminated lower continental crust? Geology 12, 1111–1114.

Xu, J.F., Castillo, P.R., 2004. Geochemical and Nd–Pb isotopic characteristics of the Tethyan asthenosphere: implications for the origin of the Indian Ocean mantle domain. Tectonophysics 393, 9–27.

Yin, A., 2000. Mode of Cenozoic east–west extension in Tibet suggests a common origin of rifts in Asia during Indo-Asian collision. J. Geophys. Res. 105, 21745–21759.

Yin, A., Harrison, T.M., 2000. Geologic evolution of the Himalayan–Tibetan orogen. Annu. Rev. Earth Planet. Sci. 28, 211–280.

Yin, A., 2006. Cenozoic tectonic evolution of the Himalayan orogen as constrained by along-strike variation of structural geometry, exhumation history, and foreland sedimentation. Earth-Sci. Rev. 76, 1–131.

Yin, J., Xu, J., Liu, C., Li, H., 1988. The Tibetan plateau: regional stratigraphic context and previous work. Philos. Trans. R. Soc. Lond. 327, 5–52.

Yuan, X., Ni, J., Kind, R., Mechie, J., Sandvol, E., 1997. Lithospheric and upper mantle structure of southern Tibet from a seismological passive source experiment. J. Geophys. Res. 102, 27491–27500.

Zhang, S.Q., Mahoney, J.J., Mo, X.X., Ghazi, A.M., Milani, L., Crawford, A.J., Guo, T.Y., Zhao, Z.D., 2005. Evidence for a widespread Tethyan upper mantle with Indian-Ocean type isotopic characteristics. J. Petrol. 46, 829–858.

Zhang, Z., Klemperer, S., 2010. Crustal structure of the Tethyan Himalaya, southern Tibet: new constraints from old wide-angle seismic data. Geophys. J. Int. 181, 1247–1260.

Zhang, Z.J., Deng, Y.F., Teng, J.W., Wang, C.Y., Gao, R., Chen, Y., Fam, W.M., 2011. An overview of the crustal structure of the Tibetan plateau after 35 years of deep seismic soundings. J. Asian Earth Sci. 40, 977–989.

Zhao, W., et al., 2001. Crustal structure of central Tibet as derived from project INDEPTH wide-angle seismic data. Geophys. J. Int. 145, 486–498.

Zhao, Z.D., Mo, X.X., Dilek, Y., Niu, Y.L., DePaolo, D.J., Robinson, P., Zhu, D.C., Sun, C.G., Dong, G.C., Zhou, S., Luo, Z.H., Hou, Z.Q., 2009. Geochemical and Sr–Nd–Pb–O isotopic compositions of the post-collisional ultrapotassic magmatism in SW Tibet: petrogenesis and implications for India intra-continental subduction beneath southern Tibet. Lithos 113, 190–212.

Zhou, S., Mo, X.X., Dong, G.C., Zhao, Z.D., Qiu, R.Z., Guo, T.Y., Wang, L.L., 2004. Ar^{40}/Ar^{39} geochronology of Cenozoic Linzizong volcanic rocks from Linzhou Basin, Tibet, China, and their geological implications. Chin. Sci. Bull. 49, 1970–1979.

Zhu, D.C., Pan, G.T., Zhao, Z.D., Lee, H.Y., Kang, Z.Q., Liao, Z.L., Wang, L.Q., Li, G.M., Dong, G.C., Liu, B., 2008. Early Cretaceous subduction-related adakite-like rocks in the Gangdese, south Tibet: products of slab melting and subsequent melt-peridotite interaction? J. Asian Earth Sci. 34, 298–309.

Zindler, A., Hart, S., 1986. Chemical geodynamics. Annu. Rev. Earth Planet. Sci. 14, 493–571.